

The external pallidum: think locally, act globally

Connor D. Courtney, Arin Pamukcu, C. Savio Chan

Department of Physiology, Feinberg School of Medicine, Northwestern University, Chicago, IL, USA

Correspondence should be addressed to C. Savio Chan, Department of Physiology, Feinberg School of Medicine, Northwestern University, 303 East Chicago Avenue, Chicago, IL 60611. saviochan@gmail.com

Running title: GPe neuron diversity & function

Keywords: cellular diversity, synaptic connectivity, motor control, Parkinson's disease

Main text: 5789 words

Text boxes: 997 words

Acknowledgments

We thank past and current members of the Chan Lab for their creativity and dedication to our understanding of the pallidum. This work was supported by NIH R01 NS069777 (CSC), R01 MH112768 (CSC), R01 NS097901 (CSC), R01 MH109466 (CSC), R01 NS088528 (CSC), and T32 AG020506 (AP).

Abstract (117 words)

The globus pallidus (GPe), as part of the basal ganglia, was once described as a black box. As its functions were unclear, the GPe has been underappreciated for decades. The advent of molecular tools has sparked a resurgence in interest in the GPe. A recent flurry of publications has unveiled the molecular landscape, synaptic organization, and functions of the GPe. It is now clear that the GPe plays multifaceted roles in both motor and non-motor functions, and is critically implicated in several motor disorders. Accordingly, the GPe should no longer be considered as a mere homogeneous relay within the so-called 'indirect pathway'. Here we summarize the key findings, challenges, consensuses, and disputes from the past few years.

Introduction (437 words)

Our ability to move is essential to survival. We and other animals produce a rich repertoire of body movements in response to internal and external cues, requiring choreographed activity across a number of brain structures. Volitional movements are thought to be controlled by two major forebrain descending pathways—the cortical and basal ganglia circuits. The general organization of the basal ganglia is conserved throughout vertebrate evolution¹. In the simplified basal ganglia circuit, the cortex provides excitatory inputs to both the striatum (dStr) and the subthalamic nucleus (STN). They in turn project to the substantia nigra pars reticulata (SNr) and internal pallidum—the output of the basal ganglia. As simplified models of the basal ganglia emphasize feedforward circuitry, intrinsic feedback circuits are often ignored (**Figure 1a**). In addition, most circuit models generally assume a homogenous neuronal population. Importantly, with the advent of molecular techniques, recent studies argue that heterogeneity of neurons in the basal ganglia is in fact a common theme²⁻¹¹.

The globus pallidus (GPe), as part of the basal ganglia, was once thought to be a simple relay nucleus. Pioneering studies using lesion and pharmacological activation yielded conflicting evidence regarding the role of the GPe in movement. Some studies reported phenotypes that were consistent with the classic basal ganglia model. For example, chemical lesions of the GPe led to a decrease in spontaneous movement¹²⁻¹⁴. In addition, selective activation of the GPe by GABA_A antagonist microinjection increased spontaneous movement¹⁵ and dyskinesias^{16,17} in monkeys. However, other work demonstrated that GPe lesions either produced no motor deficits¹⁸ or even led to increased spontaneous movement^{19,20}. Furthermore, additional work found that GPe lesions led to decreased accuracy specifically in a reaching task, but no overall motor deficits, suggesting a specific impairment in the performance of organized limb movements²¹. Similarly, non-specific stimulation of GPe neurons did not result in consistent movement outcomes^{22,23}. However, the GPe has been revealed to have a far greater complexity in a flurry of recent publications in the past few years. Historical reviews are available elsewhere²⁴⁻²⁶. We now know that the GPe has a heterogeneous neuronal makeup containing populations with distinct characteristics (**Figure 1c-e**). These neurons are believed to exert their functions via their widespread feedback projections throughout the extended basal ganglia circuits (**Figure 1b, f**). Here, we will focus on the evolving views of neuron classification in the GPe, with particular emphasis placed on the recent breakthroughs on the synaptic architecture and functions of GPe neurons. We will review evidence supporting the idea that the

unique connectivity of the GPe neuron subtypes likely drives their functions in health, and that these functions go awry in disease models.

What is a cell type? (Box 1) (457 words)

Why is 'cell type' identification important? By studying the molecular landscape and cellular composition within the GPe, researchers are able to uncover molecular markers and develop genetic tools that allow for the interrogation of organizational principles and functions of GPe neuron subtypes. Importantly, the identification of GPe neuron populations allows for experiments to be conducted on the same neuron type across subjects and laboratories. Examining the same (i.e., homologous) neuron population across species facilitates comparative studies; commonalities and differences in phenotype can then be linked to behavior.

Defining a *bona fide* functional cell type presents a challenging question. There are different grouping methods depending on the dimension of analysis and categorization of measurements. For example, the Npas1⁺ neuron class in the GPe can be classified as 'arkypallidal' and 'prototypic', depending on their respective expression of Foxp2 and Nkx2.1 (see **Box 2**). As we begin to learn about GPe neurons and their properties, the classification scheme should continue to evolve in an iterative manner.

Objectively, the classification of neurons can be based on a number of modalities, such as birthplace/date, transcriptome, connectome, intrinsic properties, involvement in behavioral and disease contexts, etc. Furthermore, complex factors also lead to biological variations in gene and protein expression within and across neuron subclasses, further obscuring distinctions between neuron subtypes. Some factors include: physiological states, experience-dependent plasticity, and the mechanisms by which local environments are modulated by neuron-glia interactions^{27–31}. In both current and past publications, we assert that PV⁺ neurons and Npas1⁺ neurons are the two principal GPe neuron classes. While we assume the expression of GPe neuron markers represents the steady state, it is possible that GPe neuron marker expression may vary temporally or in a context- or subject-specific manner. This, in addition to the limitations in transgenic models and potential age and sex differences, may explain the discrepancies in the relative numbers of GPe neuron types (and their overlap) across studies. Therefore, in addition to examining the expression of classic transcription factors, increasing knowledge about enhancer elements, terminal selectors, epigenetic modifications, and transcriptional maintenance will help refine neuron classification.

The literature has used 'subset', 'subtype', 'subclass' to describe neurons in the GPe. To date, there is no common convention in the field on how these terms should be defined. Past studies from our laboratory used 'subset' strictly as a numerical descriptor with no biological context; 'subtype' and 'type' were used interchangeably as a specific set of molecularly- or phenotypically-defined neurons; 'subclasses' as a distinct functional set of neurons that are a constituent subtype within the PV⁺ class or Npas1⁺ class, and these neurons are expected to form unique circuit modules and help achieve a complex behavioral repertoire via their respective circuit output motifs (see **Synaptic output and Functions**).

Classification of Neurons (1543 words)

Principal neuron classes

Heterogeneity in the phenotype of GPe neurons was noted in the early 1970's^{32,33}. As the descriptions of molecularly-defined GPe neuron subtypes were not established until less than a decade ago^{34,35}, it was not possible to correlate the cellular features with the molecular identity of neurons. Here, we review the consensus and disputes in our understanding of the cell identifications of GPe neurons. In addition, we outline the caveats and challenges of past studies.

The field has established that the near-exclusive expression of the calcium-binding protein parvalbumin (PV) or the transcription factor Npas1 identifies the two separate supersets of GABAergic neuron types in the adult GPe^{7,24,34-40}. PV⁺ neurons and Npas1⁺ neurons constitute 50% and 30% of the adult GPe, respectively, and are considered as the two principal neuron classes—by harnessing PV-Cre and Npas1-Cre driver lines, researchers have shown that the two neuron classes are distinct across multiple modalities, including axonal patterns, synaptic inputs, electrophysiological properties, alterations in disease states, and behavioral roles^{36-38,40-45} (**Figure 1 c-f**). The reported abundance of PV⁺ neurons across laboratories ranges from 30–60%, and their overlap with Npas1⁺ neurons within the GPe varies widely in the literature in part due to methodological differences^{34,35,39,40,42,43,46-48}. Additionally, at least some of the observed large ranges in the abundance of PV⁺ neurons is due to the spatial gradients in their distribution. However, by systematically examining a number of transgenic lines, a recent examination definitively confirmed that PV⁺ neurons account for approximately 50% of neurons in the GPe³⁶.

Neurons lacking expression of either PV or Npas1 (PV⁻-Npas1⁻ neurons) amount to 15–20% of the GPe. This population includes choline acetyltransferase-expressing (ChAT⁺) neurons, which amount to 3–5% of the total neuron population^{36,37,42}. The remaining 10–12% of GPe neurons are yet to be rigorously characterized (**Figure 1c**). This neuron population expresses the transcription factor Lhx6 (Lhx6⁺) but not Sox6 (Sox6⁻)³⁶. The identification of this unique Lhx6⁺ population corroborates data across different laboratories^{24,37,39,43}. Due to their low abundance, Lhx6⁺-Sox6⁻ neurons were likely underrepresented in previous single-cell transcriptomic data^{7,49}, and identifying reliable markers for this population of neurons has been challenging. While Lhx6⁺-Sox6⁻ neurons are unique neuron types within the GPe, they do not constitute a unique class of neurons, as Lhx6 expression is seen across PV⁺, Npas1⁺, and PV⁻-Npas1⁻ neurons within the GPe (see **Box 1**). Although it is likely that there are additional rare neuron types yet to be discovered, we now have a near-complete description of the major neuron types within the GPe. Future transcriptome-wide spatial profiling could be useful for the characterization of the rare neuron types in the GPe.

Neuron subclasses

Recent technological advancements have led to the identification of distinct subclasses of PV⁺ neurons and Npas1⁺ neurons (**Figure 1f**). Within the Npas1⁺ class, 60% are Foxp2⁺ (Npas1⁺-Foxp2⁺, also known as arky pallidal neurons); these neurons represent the first unique GPe neuron subclass to be described. Compelling data show the distinct features of Npas1⁺-Foxp2⁺ neurons, such as their developmental origin and their electrophysiological,

anatomical, and molecular profiles³⁹. As *Foxp2* expression is maintained in adults, the *Foxp2*-Cre mouse line has been successfully used across many labs to capture this population of neurons^{36,44,50,51}.

The remaining neurons within the *Npas1*⁺ class are *Nkx2.1*⁺ and *Lhx6*⁺. Importantly, *Npas1*⁺-*Nkx2.1*⁺ neurons are distinct from *Npas1*⁺-*Foxp2*⁺ neurons. Unlike *Npas1*⁺-*Foxp2*⁺ neurons that project exclusively to the dorsal striatum, the *Npas1*⁺-*Nkx2.1*⁺ neurons project to the cortex, reticular thalamic nucleus, and midbrain^{36,44} (see **Synaptic Outputs and Functions**). Accordingly, both *Npas1*⁺-*Foxp2*⁺ and *Npas1*⁺-*Nkx2.1*⁺ neuron subtypes should be regarded as *bona fide* subclasses, as recent single-cell data^{7,49} further confirmed the unique transcriptomic properties of these two *Npas1*⁺ neuron subclasses. Notably, these studies led to the identification of *Npr3*-Cre as a novel driver that captures the *Npas1*⁺-*Nkx2.1*⁺ neuron population⁴⁴, which will prove critical for further characterization of these neurons.

In addition to the two distinct *Npas1*⁺ neuron subclasses, single-cell transcriptomic data and immunolabeling suggest the existence of *PV*⁺ neuron subpopulations⁷. Multiple lines of evidence point to at least two subtypes of *PV*⁺ neurons (see also **Developmental origins**). One of these populations is identified by the marker *Kcng4*. These neurons share the electrophysiological properties, axonal projection patterns, and behavioral roles with canonical *PV*⁺ neurons⁴⁴. The most compelling data showing functionally distinct subtypes of *PV*⁺ neurons came from Lilascharoen and colleagues. They identified SNr-projecting and parafascicular thalamus (Pf)-projecting *PV*⁺ neurons; these non-overlapping sets of *PV*⁺ neurons have distinct synaptic partners, intrinsic properties, and behavioral roles⁵². Converging evidence suggests that *Lhx6* expression is weak or absent in the Pf-projecting population^{43,52}. However, it remains unclear how the current data regarding *PV*⁺ neurons intersect with each other. It will be paramount for future studies to reconcile how the axonal projection profiles align with molecular marker expression within the *PV*⁺ neuron class.

What are prototypic neurons? (Box 2) (151 words)

GPe neurons are often classified into two main groups: arky pallidal and prototypic neurons (**Figure 1d**). While recent evidence confirmed that the arky pallidal classification directly corresponds to the *Npas1*⁺-*Foxp2*⁺ neuron subclass, prototypic neurons (aka non-arky pallidal neurons) encompass a heterogeneous population of neurons from several subgroups^{7,34,35,37,39,40,42–44,47,48,53}. Immunolabeling for *Nkx2.1* is a useful approach for the identification of prototypic neurons. However, as only 90% of neurons that arise from the *Nkx2.1* lineage maintain *Nkx2.1* protein expression in adulthood, this approach is not faithful³⁶. It is important to note that all *PV*⁺ neurons are prototypic, but not all prototypic neurons are *PV*⁺. Furthermore, not all *PV*⁻ neurons are arky pallidal neurons. As the term is misused repeatedly, we propose the term prototypic be avoided, and suggest that these neurons be classified using more descriptive designations (e.g., the molecular signature) to avoid confusion.

Developmental origins

The literature converges on the idea that both the embryonic origins and the congruent expression of transcription factors govern cell specifications^{54–56}. A large set of transcription factors have been previously identified to govern the formation of the GPe^{34,35,57–61}. More recent studies have extended our understanding on the molecular landscape of the GPe and have collectively provided a firmer foundation on the neuronal identification of the GPe^{36,44}. On the other hand, neuronal birthplace has been proposed to dictate some features of GPe neuron identity³⁹. Here we review how developmental origin and molecular landscape relate to the taxonomy of GPe neurons.

The GPe primarily arises from the medial and lateral ganglionic eminence (MGE and LGE)^{34,35,39,62} (**Figure 1d**). Based on enhancer-based transgenic mice, Silberberg and colleagues⁶³ suggest the existence of two pools of PV⁺ neurons that are produced with different temporal patterns and occupy slightly different, but otherwise largely overlapping spatial domains within the GPe. While PV⁺ neurons are believed to largely arise from the MGE, only ~25% of them maintain expression of the MGE-marker Lhx6 in adulthood^{36,37}.

There have been disagreements in the earlier literature regarding the size of the Lhx6⁺ neuron population. However, recent work has yielded useful clarifications³⁶. Previous disputes arose largely due to the lack of reliable antibodies for Lhx6; past studies relied on GFP in the Lhx6-GFP mouse as a proxy for Lhx6 expression. However, one limitation with using the Lhx6-GFP mouse, which is a BAC transgenic line, is that GFP can be ectopically expressed. However, given the near-complete overlap with Nkx2.1, one can be confident that its expression is accurate within the GPe³⁶, verifying that Lhx6⁺ neurons arose from the MGE. In addition, a recent study was able to molecularly define the entirety of Lhx6⁺ neurons, thus mitigating earlier concerns regarding the Lhx6-GFP mouse line³⁶. It will be helpful to employ new markers and transgenic lines that capture unique subsets of Lhx6⁺ neurons.

Npas1⁺ neurons are derived from both the MGE and LGE^{34,35,39,40}. MGE-derived Npas1⁺ neurons are Nkx2.1⁺ and Lhx6⁺, while LGE-derived Npas1⁺ neurons are Foxp2⁺³⁶. Though developmental origins likely influence transcriptional programs that control the specifications of GPe neurons, Npas1⁺-Nkx2.1⁺ neurons and Npas1⁺-Foxp2⁺ neurons have similar electrophysiological properties³⁶. In contrast, PV⁺ neurons and Npas1⁺ neurons have striking differences in their electrophysiological and synaptic properties (see **Synaptic inputs**).

In addition to the MGE and LGE, a small fraction of GPe neurons are derived from the preoptic area (PoA)^{34,36,60,61,64}. The embryonic PoA is similar to the MGE in that it expresses the transcription factor Nkx2.1. While Dbx1⁺ neurons that originate from the PoA are known to populate the GPe^{34,60}, their properties were not fully characterized until recently^{36,64}. It is now clear that the Dbx1⁺ population contains neurons that express, to varying degrees, all established GPe neuron markers. This is consistent with the literature that PoA progenitors give rise to a small, but diverse, contingent set of neurons^{60,61}. In particular, most Dbx1⁺ neurons are Sox6⁺, and they primarily express PV⁺ (~70%) and to a lesser extent Npas1⁺ (~10%). Accordingly, Dbx1⁺ neurons do not correspond to the Lhx6⁺-Sox6⁻ population (which is PV⁻-Npas1⁻) (see **Principal neuron classes**). It is interesting to see that PV⁺-Dbx1⁺ neurons display a phenotype that is shared with the general PV⁺ population, which originates primarily from the MGE^{34,35}. Although the synaptic partners of Dbx1⁺ neurons remain to be determined, the similarities of

their intrinsic properties with canonical PV⁺ neurons is in line with previous work demonstrating that neurons that arise from spatially-distinct ontogenic domains can converge onto a single neuron class⁶⁵.

By using a progenitor-specific fate map approach, it has been shown that sonic hedgehog (Shh)-expressing progenitors from the PoA give rise to a small fraction of neurons in the GPe. This finding disambiguates the assertion from earlier studies, which conflate cumulative recombinase fate-map from a *bona fide* one⁶⁴. The significance of the robust postmitotic expression of Shh remains to be determined. As the cognate signaling receptor and signaling molecules are enriched in GPe astrocytes⁶⁶ (see also **Box 3**), it is possible that Shh is critical for cell and circuit assembly and the maintenance of cell specifications⁶⁷.

Local astrocytes support GPe functions (Box 3) (246 words)

Astrocytes are estimated to outnumber neurons by an order of magnitude⁶⁸⁻⁷⁰. They are important elements of neural circuits, where they integrate local and long-range modulatory signals through the expression of a myriad of surface receptors and transporters⁷¹⁻⁷⁴. By regulating chemical homeostasis, astrocytes are increasingly recognized to play dynamic roles in modulating neuronal and circuit activity. For example, it is believed that astrocytic regulation of GABA transmission at striatopallidal terminals is dependent on their close anatomical proximity (**Figure 2c**).

Astrocytes are highly abundant in the GPe compared to other basal ganglia nuclei⁷⁵. This abundance implies that astrocytes may play a crucial role in regulating GPe function. GPe astrocytes richly express both glutamate (GLT1 and GLAST) and GABA (GAT1 and GAT3) transporters⁷⁶⁻⁷⁹. Importantly, following chronic dopamine loss (with either 6-OHDA lesion or genetic deletion), astrocytic control of ambient glutamate is reduced due to dysregulated glutamate uptake and release, resulting in overactive striatopallidal transmission⁷⁵. In addition, an aberrant level of tonic inhibition is seen in GPe neurons following dopamine loss due to the downregulation of GAT3. Furthermore, blockade of GAT3 in the GPe impairs motor coordination in control rats⁸⁰, further suggesting functional roles for GPe astrocytes in motor control. These data highlight the importance of astrocytes in the maintenance of chemical homeostasis, and the regulation of neuronal, and circuit-level activity in the GPe, as well as the relevance of these processes in a disease condition. However, the cellular and input specificity of these regulatory processes remain to be characterized.

Synaptic Inputs (1187 words)

The classic model asserts that the GPe is an intrinsic nucleus within the basal ganglia circuit, receiving inputs exclusively from the dStr and the STN. However, accumulating evidence demonstrates that the GPe receives diverse inputs in addition to these two sources. Furthermore, the recent generation of whole-brain input maps^{36,52,53,81} reaffirm that the GPe integrates a wide variety of inputs across a number of systems and should thus no longer be considered an intrinsic nucleus. We will review the key findings from the recent studies, in particular the cell-targeting properties of these inputs. Though different markers and classification schemes are

used in the literature, the data from prototypic and arkypallidal neurons coincide with the PV⁺ vs Npas1⁺ neuron classification. For simplicity, research findings are discussed in relation to these principal neurons in the following sections.

Dorsal striatum

The dStr is, by far, the largest input to the GPe—the number of input neurons from the dStr constitutes ~80% of the total projection to the GPe and is at least an order of magnitude larger than that from other brain regions⁸¹ (**Figure 2a**). This observation is consistent with the earlier finding that GABAergic synapses amount to over 80% of all synapses in the GPe²⁵. Given the sheer volume and abundance of spiny projection neurons (SPNs), these findings are not completely surprising.

It has been known since the 1980's that axons from both dSPNs and iSPNs converge at the GPe^{82–88}. While indirect-pathway SPN (iSPN) axons terminate exclusively in the GPe, direct-pathway SPN (dSPNs) axons collateralize in both the GPe and the SNr^{82–85}. The striatofugal axons are topographically arranged, such that axons of SPNs from the medial and lateral dStr target the medial and lateral portions of their downstream targets, respectively^{81,84,86,87,89–98} (**Figure 2b**).

Previous studies showed that dSPNs provide roughly half the number of boutons compared to iSPNs in the GPe^{82,84}. However, more recent estimations of the number of boutons formed by iSPNs is three to eight times higher than that formed by dSPNs⁸¹. Both viral-tracing and patch-clamp studies demonstrate that iSPNs strongly target canonical PV⁺ neurons (i.e., STN-projecting). On the contrary, dSPNs appear to target Npas1⁺ neurons, Pf-projecting PV⁺ neurons, and ChAT⁺ neurons within the GPe^{42,44,50–52,99}. The cell-targeting properties of the dSPN input are somewhat unexpected, as earlier observations indicated that the receptors for substance P are selectively expressed in PV⁺ neurons⁴⁶. These findings altogether suggest a target-specific innervation with transmitters released from a single cell type; i.e., GABA and substance P released from dSPNs preferentially inhibit Npas1⁺ neurons and excite PV⁺ neurons, respectively. Given that Npas1⁺ neurons and PV⁺ neurons have opposite effects on motor control^{38,44}, the inhibition of Npas1⁺ neurons by GABA and excitation of PV⁺ neurons by substance P should work in concert to reinforce the same behavioral outcomes.

Subthalamic nucleus

Consistent with the literature^{100–102}, recent whole-brain inputs maps verify that the STN is one of the primary glutamatergic inputs innervating the GPe^{52,53,81}. In line with the general organization of the basal ganglia, anatomical tracing studies indicate that the STN input to the GPe is topographically organized^{10,91,103,104}. However, the cellular targeting properties of this input was not known until recently. By using *in vivo* and *ex vivo* approaches, three independent studies have convincingly demonstrated that STN inputs target PV⁺ neurons more strongly relative to Npas1⁺ neurons^{38,50,51}. Previously, the neuronal makeup of the STN was generally thought to be homogeneous^{105,106}. However, recent studies show that STN neurons are more heterogeneous than previously expected^{4,8–11}. Therefore, it will be important to determine if PV⁺-targeting neurons are distinct from those that target Npas1⁺ neurons.

Pharmacological dissection of the synaptic responses in both PV⁺ neurons and Npas1⁺ neurons confirmed that transmission at STN-GPe synapses is mediated by ionotropic glutamate receptors³⁸ as suggested by earlier studies^{107,108}. These results are consistent with prior ultrastructural studies showing that STN terminals form AMPA and NMDA receptor-containing synapses on GPe neuron dendrites^{8,109,110}.

Other extrinsic inputs

Recent studies highlight the existence of cortical inputs to the GPe^{36,111–115}. Importantly, viral-tracing data argue that the spatially-distributed cortical inputs altogether form the largest source of excitatory inputs to the GPe, contrary to the common assumption that the STN provides the largest glutamatergic input^{25,26,102,108,116–118}. Cortical inputs arise primarily from the pyramidal tract neurons³⁶. However, the precise downstream targets require further characterization, as data from recent studies are somewhat conflicting. While Karube and colleagues suggest that secondary motor cortex input selectively targets Npas1⁺-Foxp2⁺ neurons, data from others showed that cortical innervations do not support a selective targeting toward Npas1⁺-Foxp2⁺ neurons but are in fact more general^{36,52,111}.

In addition to the STN and cortex, the Pf and pedunculo-pontine nucleus are known to send glutamatergic projections to the GPe^{38,52,81,112,119–125}. These inputs do not show a biased connectivity pattern across PV⁺ neuron and Npas1⁺ neuron classes³⁸.

Whole-brain connectome analyses show that the dopaminergic input arose from the substantia nigra pars compacta, though we have yet to determine the precise neuronal subpopulation responsible^{3,52,53,81}. However, this is likely an underestimation of the total dopamine input; earlier findings suggest that a much broader area, which includes substantia nigra pars compacta, ventral tegmental area, and retrorubral area, gives rise to the dopaminergic innervations in the GPe^{11,89,126–139}. In addition to dopaminergic input, tracing studies revealed inputs from corticotropin-releasing factor-expressing (Crf⁺) neurons in the paraventricular thalamus and the central amygdala^{52,53,81,140}. Notably, the central amygdala input forms the second largest extrinsic input that targets the GPe. This projection is recently implicated in fear learning¹⁴⁰. However, the postsynaptic targets of this input remains to be explored. Strong evidence argues that PV⁺ neurons are the primary target of Crf⁺ input, as they robustly express Crfr1^{53,141}. Additionally, recent literature emphasized that PV⁺ neurons are at the intersection of motor-anxiety circuits^{53,140,141}; however, we do not currently know the downstream targets that mediate the anxiety-related response.

Local collaterals

Most, if not all, GPe neurons exhibit local axon collaterals. Juxtacellular labeling and intracellular dye-loading of GPe neurons have revealed the presence of local axon collaterals with numerous varicosities, suggesting the presence of lateral GABAergic inhibition within the GPe^{44,45,101,142–151}. Although local collaterals are integral to GPe circuit dynamics and downstream network effects¹⁵², they have not been studied in great detail due to the inherent difficulty in identifying and selectively activating individual classes of GPe neurons and their local collateral axons. However, using a combination of transgenic lines and optogenetics, researchers have recently overcome some of

the challenges associated with the interrogation of cell type-specific connectivity. Using these methods, two key findings have emerged: First, PV⁺ neurons provide the largest local input. Second, Npas1⁺-Foxp2⁺ neurons do not produce appreciable levels of local connections^{44,45,51}. As PV⁺ neuron axons arborize profusely in the STN, it is expected that deep brain stimulation, an effective surgical procedure that targets the STN as a treatment for Parkinson's disease (PD), activates these axons, altering the local network dynamics within the GPe.

Synaptic Outputs and Functions (853 words)

Although major efferent projections from the GPe have been mapped previously^{24–26}, the circuit elements involved were not known until recently. By gaining genetic access to unique neuron types within the GPe, along with other methodological advances, researchers have provided detailed circuit dissections and functional interrogations of the GPe—these studies collectively revealed that GPe neurons have the capacity to tune or maintain ongoing actions. In other words, changes in the activity of GPe neurons *in vivo* are not merely passive responses.

Consistent with the idea that PV⁺ neurons and Npas1⁺ neurons receive distinct sets of inputs, the two neuron classes have different electrophysiological properties^{36,37,44} (**Figure 1e**), suggesting a different mode of input-output transformation between them. The differences in the electrophysiological properties of neuron subclasses are more subtle, and it is still unknown how the complement of inputs varies substantially between neuron subclasses. However, *in vivo* recordings corroborate the idea of two principal neuron types in the GPe^{33,147,153,154}.

STN-projecting PV⁺ neurons promote movements

PV⁺ neurons primarily form the principal inhibitory innervation to the STN^{37,40,43,46,47,155}. Consistent with this, optogenetic and chemogenetic stimulation of pan-PV⁺ neurons or selectively STN-projecting neuron subsets promote movement^{23,52,156,157} (**Figure 3a, d**). In addition, this effect can be recapitulated by direct inhibition of STN neurons using an inhibitory opsin, GtACR2³⁸. These findings are in agreement with the well-established relationship between STN activity and movement suppression^{16,158–166}. Although earlier studies have examined the electrophysiological and anatomical properties of STN-GPe network^{100,108,116}, the cell-type specificity of the STN input in the GPe was unknown until recently. The latest findings collectively emphasize a closed reciprocal feedback loop formed between the STN and PV⁺ neurons (see **Synaptic Inputs**), adding critical insight into the cellular constituents that are involved. Furthermore, the recurrent feedback loop formed between the STN and PV⁺ neurons has strong implications on the pathological network activity observed in PD (see **Diseases Alterations**). However, it is important to note that optogenetic inhibition of PV⁺ neurons did not yield any motor responses²³, suggesting the possibility of compensatory mechanisms. Alternatively, the basal ganglia may control motor output by computation through a cascade of logic gates that operate on multiple rules. This idea is supported by the co-activation of dSPNs and iSPNs during volitional movement^{167–171}.

On the other hand, a small subset of PV⁺ neurons target the Pf. Recent data argue that these neurons are not involved in motor control, but are associated with reversal learning⁵². Given that STN-projecting and Pf-

projecting PV⁺ neurons receive distinct sets of synaptic inputs (see **Synaptic Inputs**), their roles in motor and non-motor functions, respectively, are not a complete surprise.

Npas1⁺-Foxp2⁺ neurons suppress movements

Based on relative spike timing, earlier literature infers that Npas1⁺-Foxp2⁺ neurons mediate motor inhibition by broadcasting an inhibitory signal to the dStr¹⁷². However, this causality had not been demonstrated. Recent optogenetic and chemogenetic approaches demonstrate that stimulation of Npas1⁺ neurons or Foxp2⁺ neurons leads to motor inhibition during both spontaneous ambulation and a trained-task^{38,41,44,50} (**Figure 3b**). On the contrary, optogenetic inhibition of Npas1⁺ neurons leads to motor promotion³⁸, arguing that the observed phenotype with excitatory actuators are not a spurious gain-of-function. A parallel system in the limbic basal ganglia—formed between the ventral pallidum and nucleus accumbens—has also been reported recently¹⁷³.

Despite the dense Npas1⁺-Foxp2⁺ axonal arbor within the dStr, the inhibition produced by the Npas1⁺ neurons on somatically-generated action potentials in SPNs is weak⁴¹. This mismatch suggests that additional circuit elements are involved in shaping the output of SPNs. As discussed earlier, Npas1⁺-Foxp2⁺ neurons do not form an extensive local collateral network within the GPe; it is therefore likely that they exert their circuit effects within their terminal field (i.e., within the dStr). Additionally, Npas1⁺-Foxp2⁺ axons impinge on dendrites of SPNs; however, the biological significance of this anatomical arrangement has not been examined. It is evident that a mixture of GPe neurons target striatal interneurons^{41,149,155,174}, but it remains to be determined if they are involved in motor control.

Npas1⁺-Nkx2.1⁺ neurons target the midbrain

In contrast with the projection from Npas1⁺-Foxp2⁺ neurons, the projection and function of Npas1⁺-Nkx2.1⁺ neurons are less well-characterized. These neurons project to the cortex, reticular thalamus, and the midbrain^{36,44}. However, it is unclear if a single Npas1⁺-Nkx2.1⁺ neuron projects to multiple brain regions, or if separate neurons are responsible for each of these projections.

The projection to the midbrain is in agreement with early electrophysiological, neurochemical, and viral tracing data^{175–181}. Furthermore, the molecular identity of this projection is consistent with the axonal projection patterns of Lhx6⁺ neurons^{43,182}. However, these data are at odds with the finding that PV⁺ neurons target the midbrain¹⁷⁵. It remains to be determined if Lhx6⁺-Sox6⁻ neurons contribute to this projection, or if it is constituted entirely by Npas1⁺-Nkx2.1⁺ neurons. More importantly, the behavioral relevance of this projection awaits further clarification. In particular, the feedback loop formed between GPe and midbrain dopamine neurons may create complex circuit effects (see also **Other extrinsic inputs**).

Diseases Alterations (1205 words)

Focused selection of desired actions and concomitant suppression of competing actions is key to volitional movement. Disruption of the ability to facilitate desired movements and inhibit unwanted movements results in

disorders such as PD, Huntington's disease (HD), and dystonia. As GPe neurons are critically involved in both motor promotion and suppression, we survey the emerging observations of the GPe in these disease conditions.

Parkinson's disease

The death of nigral dopamine neurons in PD leads to widespread basal ganglia circuit alterations^{183–186}. GPe neuron activity is altered following the loss of dopamine, shifting from autonomous decorrelated pacemaking to highly synchronous burst-firing activity. This aberrant GPe neuron activity correlates with the emergence of motor symptoms of PD^{187–192}, emphasizing the importance of the GPe in PD. One of the hallmarks of PD is the widespread development of synchronized basal ganglia activity known as β -oscillations (13–30 Hz), which are implicated in motor suppression^{193–197}. Recent evidence indicates that the GPe plays a critical role in the development of pathological β -oscillations. Specifically, optogenetic inhibition of GPe neurons robustly suppresses β -oscillations in 6-OHDA lesioned rats. On the other hand, optogenetic patterning of GPe neurons at β frequency leads to key circuit changes reminiscent of naturally occurring β -oscillations (**Figure 3e**). Together, these data provide strong evidence that the GPe, but not the STN or motor cortex, is required for the generation of β -oscillations¹⁹⁸.

Recent studies using animal models of PD have established that dopamine neuron loss has cell subtype-specific effects. Notably, following chronic 6-OHDA lesion, Npas1⁺ neurons display a reduction in spontaneous activity (where fast transmission was intact) *ex vivo*, whereas PV⁺ neurons are unaffected³⁷. More recent studies argue that the hypoactivity of Npas1⁺ neurons is at least in part due to changes in GABAergic signaling (see also **Box 3**) rather than alterations in their intrinsic properties³⁸. Additionally, following acute 6-OHDA administration, neither PV⁺-SNr nor PV⁺-Pf neuron subpopulations display changes in autonomous firing compared to control mice *ex vivo*⁵². This contrasts with the increased firing of PV⁺ neurons both *ex vivo* and in anesthetized mice following chronic 6-OHDA lesion¹⁹⁹. Taken together, it is likely that the firing of GPe neurons varies depending on the experimental conditions, including the timing, duration, and severity of the 6-OHDA lesion.

Synaptic inputs to GPe neurons are altered in models of PD. Following chronic 6-OHDA lesion, STN input targeting PV⁺ neurons is weakened in *ex vivo* slices. This alteration is associated with a net loss in synaptic contacts and the associated postsynaptic receptors. In contrast, STN-Npas1⁺ input is unaltered³⁸. These results are in agreement with earlier findings that AMPA and NMDA receptors are downregulated in rodent models of PD^{200,201}. Furthermore, both systemic administration and GPe-specific application of NMDA antagonists are effective in ameliorating motor symptoms in animal models of PD^{202–204}, arguing that the initial alteration may be useful for compensating the hyperactivity of STN input *in vivo*; however, the loss of NMDA receptor activity is likely maladaptive. The altered glutamate imbalance is further exacerbated by the disrupted glutamate homeostasis that is normally maintained by local astrocytes (see also **Box 3**).

In addition to the STN input, striatal input to the GPe is also altered in the chronic 6-OHDA model. An *ex vivo* examination of dStr-GPe input revealed a net increase in the strength of the total striatal input to the GPe following chronic 6-OHDA lesion⁷⁵. Although this finding is consistent with the prediction from the classic model, the observed alteration was mediated by a local disruption of glutamate homeostasis within the GPe. A more recent examination reveals that the indirect-pathway inputs to PV⁺ neurons are unchanged. This contrasts with

the direct-pathway input to Npas1⁺ neurons, which is strengthened following chronic 6-OHDA lesion⁸¹. As the ascending Npas1⁺ projections to the striatum are strengthened under the same condition⁴¹, it is likely that this recurrent loop contributes to the hypokinetic symptoms of PD. It is unclear at this point why there is a discrepancy between studies; it is worth noting that the method of stimulation (electrical vs. optogenetic) can be a key disparity.

The loss of dopamine neurons alters efferent projections and *in vivo* function of GPe neurons. Importantly, optogenetic activation of pan-PV⁺ neurons or PV⁺-SNr neurons rescues motor deficits in both acute^{23,52} and chronic³⁸ 6-OHDA animals. Following partial dopamine loss, chemogenetic inhibition of PV⁺-Pf neurons rescues impairment in a reversal learning task⁵², suggesting that PV⁺-Pf neurons may have therapeutic potential for the cognitive symptoms of PD.

Although optogenetic stimulation of PV⁺ neurons produces reliable locomotor rescue in 6-OHDA models of PD across multiple laboratories, the duration of the motor improvement varies across studies. For example, in a chronic 6-OHDA model, the motor improvement following PV⁺ neuron stimulation only lasts for the duration of the optical stimulation³⁸. However, studies using acute 6-OHDA models report motor improvements that persist beyond the duration of the optical stimulation^{23,52}, suggesting that the recovery period following 6-OHDA lesion may be of critical importance in determining whether motor-promoting effects of PV⁺ neuron stimulation are acute or persistent. Furthermore, these studies differ in the duration and intensity of their optical stimulation of PV⁺ neurons, thus making it difficult to compare results across laboratories. Therefore, it is important for future studies to carefully consider the translational applicability of different 6-OHDA lesion models and stimulation paradigms when interpreting functional results.

Huntington's disease

HD is an inherited neurodegenerative movement disorder that leads to basal ganglia dysfunction. Currently, the precise roles of GPe neurons in HD are still unclear. However, hyperactivity of the GPe is presumed to underlie some of the behavioral symptoms of HD^{205,206}, and deep brain stimulation of the GPe provides symptomatic relief in human patients²⁰⁷.

Contrary to the widespread loss of SPNs in the striatum, there is typically no GPe neuron loss in human patients until late in the disease progression^{208,209}. Consistent with this observation, GPe neuron loss is only observed at 18 months in the Q175 mouse model of HD. Although the abundance of PV⁺ neurons is maintained for up to 18 months, the abundance of Npas1⁺-Foxp2⁺ neurons is significantly reduced at 18 months, but not at 6 or 12 months²¹⁰. It will be important to determine if the susceptibility of Npas1⁺-Foxp2⁺ neurons is associated with pathological hallmarks of HD, such as neuronal intranuclear inclusions and mutant huntingtin load.

The loss of SPNs correlates with compensatory increases in $\alpha 1$, $\beta 2/3$, and $\gamma 2$ GABA_A receptor subunits on GPe neurons in human patients²¹¹. Additionally, in the Q175, YAC128, and R6/2 models of HD, there are increased postsynaptic responses to striatal inputs^{212,213}. The data from mouse models argue that the increased striatal responses are independent of cell loss in the dStr.

Dystonia

Dystonia is characterized by uncontrollable muscle contractions, resulting in involuntary and abnormal movements and postures^{214–218}. Data from animal models and human patients suggest that abnormal GPe neuron activity contributes to dystonia symptoms^{219–223}. Importantly, in the DYT1 mouse model of dystonia, there is reduced firing of spontaneously active PV⁺ neurons due to impaired function of HCN channels. Pharmacological enhancement of HCN channel gating restores physiological PV⁺ neuron pacemaking and improves motor performance²²⁴. These data suggest GPe neurons play important roles in dystonia symptomatology and highlight these neurons as potential therapeutic targets in some forms of dystonia.

Summary (Box 4) (143 words)

- Recent research has mapped the molecular landscape and the developmental origins of the GPe. We now have a near-complete catalog of the major neuron types within the GPe.
- PV⁺ neurons and Npas1⁺ neurons are the principal neuron classes in the GPe. Additionally, recent studies have provided us with a good grasp on the synaptic partners of these neurons.
- New subtypes of PV⁺ neurons and Npas1⁺ neurons have been recently identified, and are responsible for both motor and non-motor functions.
- As the GPe projects broadly and integrates a rich array of inputs, it should be considered as a key signaling hub rather than an intrinsic nucleus within the basal ganglia.
- Cell-specific alterations observed in disease models further argue that GPe neurons play critical roles in motor control and the pathophysiology of motor dysfunction. These findings provide the basis for future cell- and circuit-based therapies.

Concluding Remarks (564 words)

Important methodological advancements have propelled great strides in the studies of the GPe. Its complex neuron types and axonal projection patterns argue that the architecture of GPe does not conform to the traditional direct-indirect model of the basal ganglia. Nevertheless, our understanding of the GPe remains rather crude. While a consensus on subtypes and their functions is beginning to emerge, the expansion of our knowledge will continue to rely on cross-laboratory discoveries in an iterative manner. The goal of this review is not meant to be an exhaustive overview. Instead, we aim to summarize key findings and recent developments that fuel the next wave of discoveries that help unravel the mysteries of the GPe, while also acknowledging disagreements in the literature.

Several major gaps in knowledge should be addressed in future studies. First, the temporal organization of the activity of GPe neuron subtypes in relation to both motor and non-motor behaviors should be determined. In particular, studies that capture behavioral performance with high temporal resolution coupled with machine-learning based analysis will be extremely useful in unraveling the functional roles of GPe neuron subtypes. Additionally, correlated neural recordings and manipulations will help refine the mechanisms involved.

Next, the cellular mechanisms of GPe neuron subtypes should continue to be elucidated. For example, while it is clear that Npas1⁺-Foxp2⁺ neurons are critical for motor inhibition, the precise cellular mechanisms that underlie the behavioral response remain elusive. In addition, we have now defined Npas1⁺-Nkx2.1⁺ neurons as a unique neuron subclass; however, the activity patterns of these neurons during natural behavior is yet to be described. Furthermore, the taxonomy of PV⁺ neuron subtypes has yet to be clarified. Additional investigation of PV⁺ neuron subtypes is needed to reconcile the classifications based on separate modalities. Importantly, there now exist a set of transgenic lines that will allow the field to work together to solve more challenging questions and to reconcile discrepancies that arose from the use of suboptimal tools. Alongside this, researchers should continue to explore existing transgenic tools that would allow for genetic access to rare neuron types within the GPe, including Lhx6⁺-Sox6⁻ neurons.

Additionally, we have yet to embrace our knowledge on the richness of local chemical signaling within the GPe. The advent of optical sensors for neurotransmitters and signaling molecules (e.g., dopamine, acetylcholine, neuropeptides, neuroactive substances, etc) paves the way for advances to be made in this area. Furthermore, astrocytes (and other glia) are an integral part of the GPe; however, we have limited understanding on how they support and shape signaling of local neuronal and long-range axons (e.g., corticofugal and striatofugal axons) at the GPe and how they go awry in disease conditions.

Finally, the field as a whole should strive to reconcile differences across disease models (e.g., acute vs chronic 6-OHDA lesion; random genomic integration vs. targeted knockin). Furthermore, as nigral dopamine neurons also release Shh, brain-derived neurotrophic factor, and other trophic factors^{225,226}, it remains to be determined if toxin-animal models and human patients of PD suffer from additional complex alterations in neurochemistry following the loss of dopaminergic neurons. Therefore, it will be important in the future to specifically manipulate different nodes along these signaling cascades to pinpoint the precise signaling molecules that are crucial to proper cellular and circuit function. Until we do, there will be major challenges in distinguishing causative versus adaptive alterations in disease conditions.

References

1. Grillner, S. & El Manira, A. Current Principles of Motor Control, with Special Reference to Vertebrate Locomotion. *Physiol. Rev.* **100**, 271–320 (2020).
2. McElvain, L. E. *et al.* Specific populations of basal ganglia output neurons target distinct brain stem areas while collateralizing throughout the diencephalon. *Neuron* (2021) doi:10.1016/j.neuron.2021.03.017.
3. Poulin, J.-F. *et al.* Mapping projections of molecularly defined dopamine neuron subtypes using intersectional genetic approaches. *Nat. Neurosci.* **21**, 1260–1271 (2018).
4. Wallén-Mackenzie, Å. *et al.* Spatio-molecular domains identified in the mouse subthalamic nucleus and neighboring glutamatergic and GABAergic brain structures. *Commun. Biol.* **3**, 338 (2020).
5. Wallace, M. L. *et al.* Genetically Distinct Parallel Pathways in the Entopeduncular Nucleus for Limbic and Sensorimotor Output of the Basal Ganglia. *Neuron* **94**, 138-152.e5 (2017).

6. Miyamoto, Y. & Fukuda, T. The habenula-targeting neurons in the mouse entopeduncular nucleus contain not only somatostatin-positive neurons but also nitric oxide synthase-positive neurons. *Brain Struct. Funct.* (2021) doi:10.1007/s00429-021-02264-1.
7. Saunders, A. *et al.* Molecular Diversity and Specializations among the Cells of the Adult Mouse Brain. *Cell* **174**, 1015-1030.e16 (2018).
8. Koshimizu, Y., Fujiyama, F., Nakamura, K. C., Furuta, T. & Kaneko, T. Quantitative analysis of axon bouton distribution of subthalamic nucleus neurons in the rat by single neuron visualization with a viral vector. *J. Comp. Neurol.* **521**, 2125–2146 (2013).
9. Xiao, C. *et al.* Nicotinic receptor subtype-selective circuit patterns in the subthalamic nucleus. *J Neurosci* **35**, 3734–3746 (2015).
10. Sato, F., Parent, M., Levesque, M. & Parent, A. Axonal branching pattern of neurons of the subthalamic nucleus in primates. *J. Comp. Neurol.* **424**, 142–152 (2000).
11. Parent, A. *et al.* Organization of the basal ganglia: the importance of axonal collateralization. *Trends Neurosci.* **23**, S20-27 (2000).
12. Hauber, W., Lutz, S. & Mönkle, M. The effects of globus pallidus lesions on dopamine-dependent motor behaviour in rats. *Neuroscience* **86**, 147–157 (1998).
13. Ossowska, K., Smiałowska, M. & Wolfarth, S. A biphasic influence of globus pallidus lesions: spontaneous catalepsy followed by anticataleptic effect. *Pharmacol. Biochem. Behav.* **19**, 169–176 (1983).
14. Konitsiotis, S., Kafetzopoulos, E., Anastasopoulos, D. & Blanchet, P. J. Opposite rotation induced by dopamine agonists in rats with unilateral lesions of the globus pallidus or substantia nigra. *Behav. Brain Res.* **92**, 77–83 (1998).
15. Grabli, D. *et al.* Behavioural disorders induced by external globus pallidus dysfunction in primates: I. Behavioural study. *Brain* **127**, 2039–2054 (2004).
16. Crossman, A. R., Sambrook, M. A. & Jackson, A. Experimental hemichorea/hemiballismus in the monkey. Studies on the intracerebral site of action in a drug-induced dyskinesia. *Brain J. Neurol.* **107 (Pt 2)**, 579–596 (1984).
17. Matsumura, M., Tremblay, L., Richard, H. & Fillion, M. Activity of pallidal neurons in the monkey during dyskinesia induced by injection of bicuculline in the external pallidum. *Neuroscience* **65**, 59–70 (1995).
18. Soares, J. *et al.* Role of external pallidal segment in primate parkinsonism: comparison of the effects of 1-methyl-4-phenyl-1,2,3,6-tetrahydropyridine-induced parkinsonism and lesions of the external pallidal segment. *J Neurosci* **24**, 6417–6426 (2004).
19. Norton, S. Hyperactive behavior of rats after lesions of the globus pallidus. *Brain Res. Bull.* **1**, 193–202 (1976).
20. Joel, D. *et al.* Electrolytic lesion of globus pallidus ameliorates the behavioral and neurodegenerative effects of quinolinic acid lesion of the striatum: a potential novel treatment in a rat model of Huntington's disease. *Brain Res.* **787**, 143–148 (1998).
21. Schneider, J. S. & Olazabal, U. E. Behaviorally specific limb use deficits following globus pallidus lesions in

- rats. *Brain Res.* **308**, 341–346 (1984).
22. Anderson, M. E. & Horak, F. B. Influence of the globus pallidus on arm movements in monkeys. III. Timing of movement-related information. *J. Neurophysiol.* **54**, 433–448 (1985).
 23. Mastro, K. J. *et al.* Cell-specific pallidal intervention induces long-lasting motor recovery in dopamine-depleted mice. *Nat. Neurosci.* **20**, 815–823 (2017).
 24. Hegeman, D. J., Hong, E. S., Hernández, V. M. & Chan, C. S. The external globus pallidus: progress and perspectives. *Eur. J. Neurosci.* **43**, 1239–1265 (2016).
 25. Kita, H. Globus pallidus external segment. *Prog. Brain Res.* **160**, 111–133 (2007).
 26. Jaeger, D. & Kita, H. Functional connectivity and integrative properties of globus pallidus neurons. *Neuroscience* **198**, 44–53 (2011).
 27. Herrero-Navarro, Á. *et al.* Astrocytes and neurons share region-specific transcriptional signatures that confer regional identity to neuronal reprogramming. *Sci. Adv.* **7**, (2021).
 28. Dehorter, N. *et al.* Tuning of fast-spiking interneuron properties by an activity-dependent transcriptional switch. *Science* **349**, 1216–1220 (2015).
 29. Spitzer, N. C. Neurotransmitter Switching? No Surprise. *Neuron* **86**, 1131–1144 (2015).
 30. Spitzer, N. C. Neurotransmitter Switching in the Developing and Adult Brain. *Annu. Rev. Neurosci.* **40**, 1–19 (2017).
 31. Flavell, S. W. & Greenberg, M. E. Signaling mechanisms linking neuronal activity to gene expression and plasticity of the nervous system. *Annu. Rev. Neurosci.* **31**, 563–590 (2008).
 32. Fox, C. A., Andrade, A. N., Lu Qui, I. J. & Rafols, J. A. The primate globus pallidus: a Golgi and electron microscopic study. *J. Hirnforsch.* **15**, 75–93 (1974).
 33. DeLong, M. R. Activity of pallidal neurons during movement. *J. Neurophysiol.* **34**, 414–427 (1971).
 34. Nóbrega-Pereira, S. *et al.* Origin and molecular specification of globus pallidus neurons. *J. Neurosci. Off. J. Soc. Neurosci.* **30**, 2824–2834 (2010).
 35. Flandin, P., Kimura, S. & Rubenstein, J. L. R. The progenitor zone of the ventral medial ganglionic eminence requires Nkx2-1 to generate most of the globus pallidus but few neocortical interneurons. *J. Neurosci. Off. J. Soc. Neurosci.* **30**, 2812–2823 (2010).
 36. Abecassis, Z. A. *et al.* Npas1+-Nkx2.1+ Neurons Are an Integral Part of the Cortico-pallido-cortical Loop. *J. Neurosci* **40**, 743–768 (2020).
 37. Hernández, V. M. *et al.* Parvalbumin+ Neurons and Npas1+ Neurons Are Distinct Neuron Classes in the Mouse External Globus Pallidus. *J. Neurosci. Off. J. Soc. Neurosci.* **35**, 11830–11847 (2015).
 38. Pamukcu, A. *et al.* Parvalbumin+ and Npas1+ Pallidal Neurons Have Distinct Circuit Topology and Function. *J. Neurosci. Off. J. Soc. Neurosci.* **40**, 7855–7876 (2020).
 39. Dodson, P. D. *et al.* Distinct developmental origins manifest in the specialized encoding of movement by adult neurons of the external globus pallidus. *Neuron* **86**, 501–513 (2015).
 40. Abdi, A. *et al.* Prototypic and arkypallidal neurons in the dopamine-intact external globus pallidus. *J. Neurosci. Off. J. Soc. Neurosci.* **35**, 6667–6688 (2015).

41. Glajch, K. E. *et al.* Npas1+ Pallidal Neurons Target Striatal Projection Neurons. *J. Neurosci. Off. J. Soc. Neurosci.* **36**, 5472–5488 (2016).
42. Saunders, A. *et al.* A direct GABAergic output from the basal ganglia to frontal cortex. *Nature* **521**, 85–89 (2015).
43. Mastro, K. J., Bouchard, R. S., Holt, H. A. K. & Gittis, A. H. Transgenic mouse lines subdivide external segment of the globus pallidus (GPe) neurons and reveal distinct GPe output pathways. *J. Neurosci. Off. J. Soc. Neurosci.* **34**, 2087–2099 (2014).
44. Cui, Q. *et al.* Dissociable Roles of Pallidal Neuron Subtypes in Regulating Motor Patterns. *J. Neurosci. Off. J. Soc. Neurosci.* (2021) doi:10.1523/JNEUROSCI.2210-20.2021.
45. Higgs, M. H., Jones, J. A., Chan, C. S. & Wilson, C. J. Periodic unitary synaptic currents in the mouse globus pallidus during spontaneous firing in slices. *J. Neurophysiol.* **125**, 1482–1500 (2021).
46. Mizutani, K., Takahashi, S., Okamoto, S., Karube, F. & Fujiyama, F. Substance P effects exclusively on prototypic neurons in mouse globus pallidus. *Brain Struct. Funct.* **222**, 4089–4110 (2017).
47. Oh, Y.-M. *et al.* Using a novel PV-Cre rat model to characterize pallidonigral cells and their terminations. *Brain Struct. Funct.* **222**, 2359–2378 (2017).
48. Abrahao, K. P. & Lovinger, D. M. Classification of GABAergic neuron subtypes from the globus pallidus using wild-type and transgenic mice. *J. Physiol.* **596**, 4219–4235 (2018).
49. Zeisel, A. *et al.* Molecular Architecture of the Mouse Nervous System. *Cell* **174**, 999–1014.e22 (2018).
50. Aristieta, A. *et al.* A Disynaptic Circuit in the Globus Pallidus Controls Locomotion Inhibition. *Curr. Biol. CB* **31**, 707–721.e7 (2021).
51. Ketzef, M. & Silberberg, G. Differential Synaptic Input to External Globus Pallidus Neuronal Subpopulations In Vivo. *Neuron* **109**, 516–529.e4 (2021).
52. Lilascharoen, V. *et al.* Divergent pallidal pathways underlying distinct Parkinsonian behavioral deficits. *Nat. Neurosci.* **24**, 504–515 (2021).
53. Hunt, A. J. *et al.* Paraventricular hypothalamic and amygdalar CRF neurons synapse in the external globus pallidus. *Brain Struct. Funct.* **223**, 2685–2698 (2018).
54. Hu, J. S., Vogt, D., Sandberg, M. & Rubenstein, J. L. Cortical interneuron development: a tale of time and space. *Dev. Camb. Engl.* **144**, 3867–3878 (2017).
55. Lim, L., Mi, D., Llorca, A. & Marín, O. Development and Functional Diversification of Cortical Interneurons. *Neuron* **100**, 294–313 (2018).
56. Fishell, G. & Kepecs, A. Interneuron Types as Attractors and Controllers. *Annu. Rev. Neurosci.* **43**, 1–30 (2020).
57. Kohtz, J. D., Baker, D. P., Corte, G. & Fishell, G. Regionalization within the mammalian telencephalon is mediated by changes in responsiveness to Sonic Hedgehog. *Dev. Camb. Engl.* **125**, 5079–5089 (1998).
58. Sussel, L., Marin, O., Kimura, S. & Rubenstein, J. L. Loss of Nkx2.1 homeobox gene function results in a ventral to dorsal molecular respecification within the basal telencephalon: evidence for a transformation of the pallidum into the striatum. *Dev. Camb. Engl.* **126**, 3359–3370 (1999).

59. Long, J. E., Cobos, I., Potter, G. B. & Rubenstein, J. L. R. Dlx1&2 and Mash1 transcription factors control MGE and CGE patterning and differentiation through parallel and overlapping pathways. *Cereb. Cortex N. Y. N 1991* **19 Suppl 1**, i96-106 (2009).
60. Gelman, D. M. *et al.* The embryonic preoptic area is a novel source of cortical GABAergic interneurons. *J. Neurosci. Off. J. Soc. Neurosci.* **29**, 9380–9389 (2009).
61. Gelman, D. *et al.* A wide diversity of cortical GABAergic interneurons derives from the embryonic preoptic area. *J. Neurosci. Off. J. Soc. Neurosci.* **31**, 16570–16580 (2011).
62. Chen, Y.-J. J. *et al.* Single-cell RNA sequencing identifies distinct mouse medial ganglionic eminence cell types. *Sci. Rep.* **7**, 45656 (2017).
63. Silberberg, S. N. *et al.* Subpallial Enhancer Transgenic Lines: a Data and Tool Resource to Study Transcriptional Regulation of GABAergic Cell Fate. *Neuron* **92**, 59–74 (2016).
64. Poulin, J.-F. *et al.* PRISM: A Progenitor-Restricted Intersectional Fate Mapping Approach Redefines Forebrain Lineages. *Dev. Cell* **53**, 740-753.e3 (2020).
65. Chittajallu, R. *et al.* Dual origins of functionally distinct O-LM interneurons revealed by differential 5-HT(3A)R expression. *Nat. Neurosci.* **16**, 1598–1607 (2013).
66. Garcia, A. D. R., Petrova, R., Eng, L. & Joyner, A. L. Sonic hedgehog regulates discrete populations of astrocytes in the adult mouse forebrain. *J. Neurosci. Off. J. Soc. Neurosci.* **30**, 13597–13608 (2010).
67. Fuccillo, M., Joyner, A. L. & Fishell, G. Morphogen to mitogen: the multiple roles of hedgehog signalling in vertebrate neural development. *Nat. Rev. Neurosci.* **7**, 772–783 (2006).
68. Salvesen, L. *et al.* Changes in total cell numbers of the basal ganglia in patients with multiple system atrophy - A stereological study. *Neurobiol. Dis.* **74**, 104–113 (2015).
69. Lange, H., Thörner, G., Hopf, A. & Schröder, K. F. Morphometric studies of the neuropathological changes in choreatic diseases. *J. Neurol. Sci.* **28**, 401–425 (1976).
70. Karlsen, A. S. & Pakkenberg, B. Total numbers of neurons and glial cells in cortex and basal ganglia of aged brains with Down syndrome--a stereological study. *Cereb. Cortex N. Y. N 1991* **21**, 2519–2524 (2011).
71. Theodosis, D. T., Poulain, D. A. & Oliet, S. H. R. Activity-dependent structural and functional plasticity of astrocyte-neuron interactions. *Physiol. Rev.* **88**, 983–1008 (2008).
72. Perea, G., Navarrete, M. & Araque, A. Tripartite synapses: astrocytes process and control synaptic information. *Trends Neurosci.* **32**, 421–431 (2009).
73. Nedergaard, M. & Verkhratsky, A. Artifact versus reality--how astrocytes contribute to synaptic events. *Glia* **60**, 1013–1023 (2012).
74. Araque, A. *et al.* Gliotransmitters travel in time and space. *Neuron* **81**, 728–739 (2014).
75. Cui, Q. *et al.* Blunted mGluR Activation Disinhibits Striatopallidal Transmission in Parkinsonian Mice. *Cell Rep.* **17**, 2431–2444 (2016).
76. Furuta, A., Rothstein, J. D. & Martin, L. J. Glutamate transporter protein subtypes are expressed differentially during rat CNS development. *J. Neurosci. Off. J. Soc. Neurosci.* **17**, 8363–8375 (1997).
77. Scimemi, A. Structure, function, and plasticity of GABA transporters. *Front. Cell. Neurosci.* **8**, 161 (2014).

78. Jin, X.-T., Galvan, A., Wichmann, T. & Smith, Y. Localization and Function of GABA Transporters GAT-1 and GAT-3 in the Basal Ganglia. *Front. Syst. Neurosci.* **5**, 63 (2011).
79. Galvan, A., Hu, X., Smith, Y. & Wichmann, T. Localization and function of GABA transporters in the globus pallidus of parkinsonian monkeys. *Exp. Neurol.* **223**, 505–515 (2010).
80. Chazalon, M. *et al.* GAT-3 Dysfunction Generates Tonic Inhibition in External Globus Pallidus Neurons in Parkinsonian Rodents. *Cell Rep.* **23**, 1678–1690 (2018).
81. Cui, Q. *et al.* Striatal Direct Pathway Targets Npas1+ Pallidal Neurons. *J. Neurosci. Off. J. Soc. Neurosci.* (2021) doi:10.1523/JNEUROSCI.2306-20.2021.
82. Kawaguchi, Y., Wilson, C. J. & Emson, P. C. Projection subtypes of rat neostriatal matrix cells revealed by intracellular injection of biocytin. *J. Neurosci. Off. J. Soc. Neurosci.* **10**, 3421–3438 (1990).
83. Wu, Y., Richard, S. & Parent, A. The organization of the striatal output system: a single-cell juxtacellular labeling study in the rat. *Neurosci. Res.* **38**, 49–62 (2000).
84. Fujiyama, F. *et al.* Exclusive and common targets of neostriatofugal projections of rat striosome neurons: a single neuron-tracing study using a viral vector. *Eur. J. Neurosci.* **33**, 668–677 (2011).
85. Lévesque, M. & Parent, A. The striatofugal fiber system in primates: a reevaluation of its organization based on single-axon tracing studies. *Proc. Natl. Acad. Sci. U. S. A.* **102**, 11888–11893 (2005).
86. Okamoto, S. *et al.* Overlapping Projections of Neighboring Direct and Indirect Pathway Neostriatal Neurons to Globus Pallidus External Segment. *iScience* 101409 (2020) doi:10.1016/j.isci.2020.101409.
87. Chang, H. T., Wilson, C. J. & Kitai, S. T. Single neostriatal efferent axons in the globus pallidus: a light and electron microscopic study. *Science* **213**, 915–918 (1981).
88. Cazorla, M. *et al.* Dopamine D2 receptors regulate the anatomical and functional balance of basal ganglia circuitry. *Neuron* **81**, 153–164 (2014).
89. Hedreen, J. C. & DeLong, M. R. Organization of striatopallidal, striatonigral, and nigrostriatal projections in the macaque. *J. Comp. Neurol.* **304**, 569–595 (1991).
90. Deniau, J. M., Menetrey, A. & Charpier, S. The lamellar organization of the rat substantia nigra pars reticulata: segregated patterns of striatal afferents and relationship to the topography of corticostriatal projections. *Neuroscience* **73**, 761–781 (1996).
91. Nambu, A. Somatotopic organization of the primate Basal Ganglia. *Front. Neuroanat.* **5**, 26 (2011).
92. Romanelli, P., Esposito, V., Schaal, D. W. & Heit, G. Somatotopy in the basal ganglia: experimental and clinical evidence for segregated sensorimotor channels. *Brain Res. Brain Res. Rev.* **48**, 112–128 (2005).
93. Bertino, S. *et al.* Spatially coherent and topographically organized pathways of the human globus pallidus. *Hum. Brain Mapp.* **41**, 4641–4661 (2020).
94. Lee, J., Wang, W. & Sabatini, B. L. Anatomically segregated basal ganglia pathways allow parallel behavioral modulation. *Nat. Neurosci.* **23**, 1388–1398 (2020).
95. Cowan, W. M. & Powell, T. P. Strio-pallidal projection in the monkey. *J. Neurol. Neurosurg. Psychiatry* **29**, 426–439 (1966).
96. Wilson, C. J. & Phelan, K. D. Dual topographic representation of neostriatum in the globus pallidus of rats.

- Brain Res.* **243**, 354–359 (1982).
97. Foster, N. N. *et al.* *The mouse cortico-basal ganglia-thalamic network.* <http://biorxiv.org/lookup/doi/10.1101/2020.10.06.326876> (2020) doi:10.1101/2020.10.06.326876.
 98. Heilbronner, S. R., Meyer, M. A. A., Choi, E. Y. & Haber, S. N. How do cortico-striatal projections impact on downstream pallidal circuitry? *Brain Struct. Funct.* **223**, 2809–2821 (2018).
 99. Yuan, X.-S. *et al.* Striatal adenosine A2A receptor neurons control active-period sleep via parvalbumin neurons in external globus pallidus. *eLife* **6**, (2017).
 100. Robledo, P. & Féger, J. Excitatory influence of rat subthalamic nucleus to substantia nigra pars reticulata and the pallidal complex: electrophysiological data. *Brain Res.* **518**, 47–54 (1990).
 101. Kita, H. & Kitai, S. T. The morphology of globus pallidus projection neurons in the rat: an intracellular staining study. *Brain Res.* **636**, 308–319 (1994).
 102. Smith, Y., Bevan, M. D., Shink, E. & Bolam, J. P. Microcircuitry of the direct and indirect pathways of the basal ganglia. *Neuroscience* **86**, 353–387 (1998).
 103. Iwamuro, H. Electrophysiological evidences of organization of cortical motor information in the Basal Ganglia. *J. Mov. Disord.* **4**, 8–12 (2011).
 104. Baufreton, J. *et al.* Sparse but selective and potent synaptic transmission from the globus pallidus to the subthalamic nucleus. *J. Neurophysiol.* **102**, 532–545 (2009).
 105. Yelnik, J. & Percheron, G. Subthalamic neurons in primates: a quantitative and comparative analysis. *Neuroscience* **4**, 1717–1743 (1979).
 106. Hammond, C. & Yelnik, J. Intracellular labelling of rat subthalamic neurones with horseradish peroxidase: computer analysis of dendrites and characterization of axon arborization. *Neuroscience* **8**, 781–790 (1983).
 107. Kita, H. Responses of globus pallidus neurons to cortical stimulation: intracellular study in the rat. *Brain Res.* **589**, 84–90 (1992).
 108. Kita, H. & Kitai, S. T. Intracellular study of rat globus pallidus neurons: membrane properties and responses to neostriatal, subthalamic and nigral stimulation. *Brain Res.* **564**, 296–305 (1991).
 109. Bernard, V. & Bolam, J. P. Subcellular and subsynaptic distribution of the NR1 subunit of the NMDA receptor in the neostriatum and globus pallidus of the rat: co-localization at synapses with the GluR2/3 subunit of the AMPA receptor. *Eur. J. Neurosci.* **10**, 3721–3736 (1998).
 110. Clarke, N. P. & Bolam, J. P. Distribution of glutamate receptor subunits at neurochemically characterized synapses in the entopeduncular nucleus and subthalamic nucleus of the rat. *J. Comp. Neurol.* **397**, 403–420 (1998).
 111. Karube, F., Takahashi, S., Kobayashi, K. & Fujiyama, F. Motor cortex can directly drive the globus pallidus neurons in a projection neuron type-dependent manner in the rat. *eLife* **8**, (2019).
 112. Naito, A. & Kita, H. The cortico-pallidal projection in the rat: an anterograde tracing study with biotinylated dextran amine. *Brain Res.* **653**, 251–257 (1994).
 113. Adkins, R. S. *et al.* A multimodal cell census and atlas of the mammalian primary motor cortex. *bioRxiv* 2020.10.19.343129 (2020) doi:10.1101/2020.10.19.343129.

114. Garcia, A. F., Crummy, E. A., Webb, I. G., Nooney, M. N. & Ferguson, S. M. Distinct populations of cortical pyramidal neurons mediate drug reward and aversion. *Nat. Commun.* **12**, 182 (2021).
115. Muñoz-Castañeda, R. *et al.* *Cellular Anatomy of the Mouse Primary Motor Cortex*. <http://biorxiv.org/lookup/doi/10.1101/2020.10.02.323154> (2020) doi:10.1101/2020.10.02.323154.
116. Kita, H. & Kitai, S. T. Efferent projections of the subthalamic nucleus in the rat: light and electron microscopic analysis with the PHA-L method. *J. Comp. Neurol.* **260**, 435–452 (1987).
117. Nambu, A. *et al.* Excitatory cortical inputs to pallidal neurons via the subthalamic nucleus in the monkey. *J. Neurophysiol.* **84**, 289–300 (2000).
118. Parent, A. & Hazrati, L. N. Functional anatomy of the basal ganglia. II. The place of subthalamic nucleus and external pallidum in basal ganglia circuitry. *Brain Res. Brain Res. Rev.* **20**, 128–154 (1995).
119. Parent, M. & Parent, A. Single-axon tracing and three-dimensional reconstruction of centre median-parafascicular thalamic neurons in primates. *J. Comp. Neurol.* **481**, 127–144 (2005).
120. Kincaid, A. E., Penney, J. B., Young, A. B. & Newman, S. W. The globus pallidus receives a projection from the parafascicular nucleus in the rat. *Brain Res.* **553**, 18–26 (1991).
121. Deschênes, M., Bourassa, J., Doan, V. D. & Parent, A. A single-cell study of the axonal projections arising from the posterior intralaminar thalamic nuclei in the rat. *Eur. J. Neurosci.* **8**, 329–343 (1996).
122. Sadikot, A. F., Parent, A., Smith, Y. & Bolam, J. P. Efferent connections of the centromedian and parafascicular thalamic nuclei in the squirrel monkey: a light and electron microscopic study of the thalamostriatal projection in relation to striatal heterogeneity. *J. Comp. Neurol.* **320**, 228–242 (1992).
123. Yasukawa, T., Kita, T., Xue, Y. & Kita, H. Rat intralaminar thalamic nuclei projections to the globus pallidus: a biotinylated dextran amine anterograde tracing study. *J. Comp. Neurol.* **471**, 153–167 (2004).
124. Kita, H., Nambu, A., Kaneda, K., Tachibana, Y. & Takada, M. Role of ionotropic glutamatergic and GABAergic inputs on the firing activity of neurons in the external pallidum in awake monkeys. *J. Neurophysiol.* **92**, 3069–3084 (2004).
125. Mouroux, M., Hassani, O. K. & Féger, J. Electrophysiological and Fos immunohistochemical evidence for the excitatory nature of the parafascicular projection to the globus pallidus. *Neuroscience* **81**, 387–397 (1997).
126. Charara, A. & Parent, A. Brainstem dopaminergic, cholinergic and serotonergic afferents to the pallidum in the squirrel monkey. *Brain Res.* **640**, 155–170 (1994).
127. Lindvall, O. & Björklund, A. Dopaminergic innervation of the globus pallidus by collaterals from the nigrostriatal pathway. *Brain Res.* **172**, 169–173 (1979).
128. Smith, Y., Lavoie, B., Dumas, J. & Parent, A. Evidence for a distinct nigropallidal dopaminergic projection in the squirrel monkey. *Brain Res.* **482**, 381–386 (1989).
129. Gauthier, J., Parent, M., Lévesque, M. & Parent, A. The axonal arborization of single nigrostriatal neurons in rats. *Brain Res.* **834**, 228–232 (1999).
130. Debeir, T. *et al.* Effect of intrastriatal 6-OHDA lesion on dopaminergic innervation of the rat cortex and globus pallidus. *Exp. Neurol.* **193**, 444–454 (2005).
131. Cossette, M., Lévesque, M. & Parent, A. Extrastriatal dopaminergic innervation of human basal ganglia.

- Neurosci. Res.* **34**, 51–54 (1999).
132. Lavoie, B., Smith, Y. & Parent, A. Dopaminergic innervation of the basal ganglia in the squirrel monkey as revealed by tyrosine hydroxylase immunohistochemistry. *J. Comp. Neurol.* **289**, 36–52 (1989).
133. Prensa, L. & Parent, A. The nigrostriatal pathway in the rat: A single-axon study of the relationship between dorsal and ventral tier nigral neurons and the striosome/matrix striatal compartments. *J. Neurosci. Off. J. Soc. Neurosci.* **21**, 7247–7260 (2001).
134. Prensa, L., Cossette, M. & Parent, A. Dopaminergic innervation of human basal ganglia. *J. Chem. Neuroanat.* **20**, 207–213 (2000).
135. Jan, C. *et al.* Dopaminergic innervation of the pallidum in the normal state, in MPTP-treated monkeys and in parkinsonian patients. *Eur. J. Neurosci.* **12**, 4525–4535 (2000).
136. Dopeso-Reyes, I. G. *et al.* Calbindin content and differential vulnerability of midbrain efferent dopaminergic neurons in macaques. *Front. Neuroanat.* **8**, 146 (2014).
137. Parent, A. & Smith, Y. Differential dopaminergic innervation of the two pallidal segments in the squirrel monkey (*Saimiri sciureus*). *Brain Res.* **426**, 397–400 (1987).
138. Smith, Y. & Villalba, R. Striatal and extrastriatal dopamine in the basal ganglia: an overview of its anatomical organization in normal and Parkinsonian brains. *Mov. Disord. Off. J. Mov. Disord. Soc.* **23 Suppl 3**, S534-547 (2008).
139. Anaya-Martinez, V., Martinez-Marcos, A., Martinez-Fong, D., Aceves, J. & Erij, D. Substantia nigra compacta neurons that innervate the reticular thalamic nucleus in the rat also project to striatum or globus pallidus: implications for abnormal motor behavior. *Neuroscience* **143**, 477–486 (2006).
140. Giovanniello, J. *et al.* A Central Amygdala-Globus Pallidus Circuit Conveys Unconditioned Stimulus-Related Information and Controls Fear Learning. *J. Neurosci. Off. J. Soc. Neurosci.* **40**, 9043–9054 (2020).
141. Sztainberg, Y., Kuperman, Y., Justice, N. & Chen, A. An anxiolytic role for CRF receptor type 1 in the globus pallidus. *J. Neurosci. Off. J. Soc. Neurosci.* **31**, 17416–17424 (2011).
142. Fujiyama, F. *et al.* A single-neuron tracing study of arky pallidal and prototypic neurons in healthy rats. *Brain Struct. Funct.* **221**, 4733–4740 (2016).
143. Okoyama, S., Nakamura, Y., Moriizumi, T. & Kitao, Y. Electron microscopic analysis of the synaptic organization of the globus pallidus in the cat. *J. Comp. Neurol.* **265**, 323–331 (1987).
144. Millhouse, O. E. Pallidal neurons in the rat. *J. Comp. Neurol.* **254**, 209–227 (1986).
145. Kita, H. Parvalbumin-immunopositive neurons in rat globus pallidus: a light and electron microscopic study. *Brain Res.* **657**, 31–41 (1994).
146. Sadek, A. R., Magill, P. J. & Bolam, J. P. A single-cell analysis of intrinsic connectivity in the rat globus pallidus. *J. Neurosci. Off. J. Soc. Neurosci.* **27**, 6352–6362 (2007).
147. Mallet, N. *et al.* Dichotomous organization of the external globus pallidus. *Neuron* **74**, 1075–1086 (2012).
148. Nambu, A. & Llinás, R. Morphology of globus pallidus neurons: its correlation with electrophysiology in guinea pig brain slices. *J. Comp. Neurol.* **377**, 85–94 (1997).
149. Bevan, M. D., Booth, P. A., Eaton, S. A. & Bolam, J. P. Selective innervation of neostriatal interneurons by a

- subclass of neuron in the globus pallidus of the rat. *J. Neurosci. Off. J. Soc. Neurosci.* **18**, 9438–9452 (1998).
150. Sato, F., Lavallée, P., Lévesque, M. & Parent, A. Single-axon tracing study of neurons of the external segment of the globus pallidus in primate. *J. Comp. Neurol.* **417**, 17–31 (2000).
151. Bugaysen, J., Bar-Gad, I. & Korngreen, A. Continuous modulation of action potential firing by a unitary GABAergic connection in the globus pallidus in vitro. *J. Neurosci. Off. J. Soc. Neurosci.* **33**, 12805–12809 (2013).
152. Terman, D., Rubin, J. E., Yew, A. C. & Wilson, C. J. Activity patterns in a model for the subthalamopallidal network of the basal ganglia. *J. Neurosci. Off. J. Soc. Neurosci.* **22**, 2963–2976 (2002).
153. Yoshida, A. & Tanaka, M. Two Types of Neurons in the Primate Globus Pallidus External Segment Play Distinct Roles in Antisaccade Generation. *Cereb. Cortex N. Y. N 1991* **26**, 1187–1199 (2016).
154. Mink, J. W. & Thach, W. T. Basal ganglia motor control. I. Nonexclusive relation of pallidal discharge to five movement modes. *J. Neurophysiol.* **65**, 273–300 (1991).
155. Saunders, A., Huang, K. W. & Sabatini, B. L. Globus Pallidus Externus Neurons Expressing parvalbumin Interconnect the Subthalamic Nucleus and Striatal Interneurons. *PLoS One* **11**, e0149798 (2016).
156. Pamukcu, A. *et al.* Parvalbumin+ and Npas1+ Pallidal Neurons Have Distinct Circuit Topology and Function. *J. Neurosci. Off. J. Soc. Neurosci.* **40**, 7855–7876 (2020).
157. Assaf, F. & Schiller, Y. A chemogenetic approach for treating experimental Parkinson's disease. *Mov. Disord. Off. J. Mov. Disord. Soc.* **34**, 469–479 (2019).
158. Wessel, J. R. & Aron, A. R. On the Globality of Motor Suppression: Unexpected Events and Their Influence on Behavior and Cognition. *Neuron* **93**, 259–280 (2017).
159. Fife, K. H. *et al.* Causal role for the subthalamic nucleus in interrupting behavior. *eLife* **6**, (2017).
160. Schmidt, R., Leventhal, D. K., Mallet, N., Chen, F. & Berke, J. D. Canceling actions involves a race between basal ganglia pathways. *Nat. Neurosci.* **16**, 1118–1124 (2013).
161. Hamani, C., Saint-Cyr, J. A., Fraser, J., Kaplitt, M. & Lozano, A. M. The subthalamic nucleus in the context of movement disorders. *Brain J. Neurol.* **127**, 4–20 (2004).
162. Aron, A. R. *et al.* Converging evidence for a fronto-basal-ganglia network for inhibitory control of action and cognition. *J. Neurosci. Off. J. Soc. Neurosci.* **27**, 11860–11864 (2007).
163. Aron, A. R. & Poldrack, R. A. Cortical and subcortical contributions to Stop signal response inhibition: role of the subthalamic nucleus. *J. Neurosci. Off. J. Soc. Neurosci.* **26**, 2424–2433 (2006).
164. Eagle, D. M. *et al.* Stop-signal reaction-time task performance: role of prefrontal cortex and subthalamic nucleus. *Cereb. Cortex N. Y. N 1991* **18**, 178–188 (2008).
165. Schweizer, N. *et al.* Limiting glutamate transmission in a Vglut2-expressing subpopulation of the subthalamic nucleus is sufficient to cause hyperlocomotion. *Proc. Natl. Acad. Sci. U. S. A.* **111**, 7837–7842 (2014).
166. Adam, E. M., Johns, T. & Sur, M. *Cortico-subthalamic projections send brief stop signals to halt visually-guided locomotion.* <http://biorxiv.org/lookup/doi/10.1101/2020.02.05.936443> (2020) doi:10.1101/2020.02.05.936443.
167. Cui, G. *et al.* Concurrent activation of striatal direct and indirect pathways during action initiation. *Nature*

- 494, 238–242 (2013).
168. Parker, J. G. *et al.* Diametric neural ensemble dynamics in parkinsonian and dyskinetic states. *Nature* **557**, 177–182 (2018).
169. Markowitz, J. E. *et al.* The Striatum Organizes 3D Behavior via Moment-to-Moment Action Selection. *Cell* **174**, 44–58.e17 (2018).
170. Tecuapetla, F., Matias, S., Dugue, G. P., Mainen, Z. F. & Costa, R. M. Balanced activity in basal ganglia projection pathways is critical for contraversive movements. *Nat. Commun.* **5**, 4315 (2014).
171. Tecuapetla, F., Jin, X., Lima, S. Q. & Costa, R. M. Complementary Contributions of Striatal Projection Pathways to Action Initiation and Execution. *Cell* **166**, 703–715 (2016).
172. Mallet, N. *et al.* Arky pallidal Cells Send a Stop Signal to Striatum. *Neuron* **89**, 308–316 (2016).
173. Vachez, Y. M. *et al.* Ventral arky pallidal neurons inhibit accumbal firing to promote reward consumption. *Nat. Neurosci.* **24**, 379–390 (2021).
174. Corbit, V. L. *et al.* Pallidostriatal Projections Promote β Oscillations in a Dopamine-Depleted Biophysical Network Model. *J. Neurosci. Off. J. Soc. Neurosci.* **36**, 5556–5571 (2016).
175. Beier, K. T. *et al.* Rabies screen reveals GPe control of cocaine-triggered plasticity. *Nature* **549**, 345–350 (2017).
176. Watabe-Uchida, M., Zhu, L., Ogawa, S. K., Vamanrao, A. & Uchida, N. Whole-brain mapping of direct inputs to midbrain dopamine neurons. *Neuron* **74**, 858–873 (2012).
177. Lee, C. R., Abercrombie, E. D. & Tepper, J. M. Pallidal control of substantia nigra dopaminergic neuron firing pattern and its relation to extracellular neostriatal dopamine levels. *Neuroscience* **129**, 481–489 (2004).
178. Cobb, W. S. & Abercrombie, E. D. Relative involvement of globus pallidus and subthalamic nucleus in the regulation of somatodendritic dopamine release in substantia nigra is dopamine-dependent. *Neuroscience* **119**, 777–786 (2003).
179. Paladini, C. A., Celada, P. & Tepper, J. M. Striatal, pallidal, and pars reticulata evoked inhibition of nigrostriatal dopaminergic neurons is mediated by GABA(A) receptors in vivo. *Neuroscience* **89**, 799–812 (1999).
180. Celada, P., Paladini, C. A. & Tepper, J. M. GABAergic control of rat substantia nigra dopaminergic neurons: role of globus pallidus and substantia nigra pars reticulata. *Neuroscience* **89**, 813–825 (1999).
181. Brazhnik, E., Shah, F. & Tepper, J. M. GABAergic afferents activate both GABAA and GABAB receptors in mouse substantia nigra dopaminergic neurons in vivo. *J. Neurosci. Off. J. Soc. Neurosci.* **28**, 10386–10398 (2008).
182. Evans, R. C. *et al.* Functional Dissection of Basal Ganglia Inhibitory Inputs onto Substantia Nigra Dopaminergic Neurons. *Cell Rep.* **32**, 108156 (2020).
183. McGregor, M. M. & Nelson, A. B. Circuit Mechanisms of Parkinson’s Disease. *Neuron* **101**, 1042–1056 (2019).
184. Albin, R. L., Young, A. B. & Penney, J. B. The functional anatomy of disorders of the basal ganglia. *Trends Neurosci.* **18**, 63–64 (1995).

185. DeLong, M. R. Primate models of movement disorders of basal ganglia origin. *Trends Neurosci.* **13**, 281–285 (1990).
186. Bergman, H. *et al.* Physiological aspects of information processing in the basal ganglia of normal and parkinsonian primates. *Trends Neurosci.* **21**, 32–38 (1998).
187. Dwi Wahyu, I., Chiken, S., Hasegawa, T., Sano, H. & Nambu, A. Abnormal Cortico-Basal Ganglia Neurotransmission in a Mouse Model of L-DOPA-Induced Dyskinesia. *J. Neurosci. Off. J. Soc. Neurosci.* **41**, 2668–2683 (2021).
188. Fillion, M. & Tremblay, L. Abnormal spontaneous activity of globus pallidus neurons in monkeys with MPTP-induced parkinsonism. *Brain Res.* **547**, 142–151 (1991).
189. Nini, A., Feingold, A., Slovin, H. & Bergman, H. Neurons in the globus pallidus do not show correlated activity in the normal monkey, but phase-locked oscillations appear in the MPTP model of parkinsonism. *J. Neurophysiol.* **74**, 1800–1805 (1995).
190. Raz, A., Vaadia, E. & Bergman, H. Firing patterns and correlations of spontaneous discharge of pallidal neurons in the normal and the tremulous 1-methyl-4-phenyl-1,2,3,6-tetrahydropyridine vervet model of parkinsonism. *J. Neurosci. Off. J. Soc. Neurosci.* **20**, 8559–8571 (2000).
191. Magill, P. J., Bolam, J. P. & Bevan, M. D. Dopamine regulates the impact of the cerebral cortex on the subthalamic nucleus-globus pallidus network. *Neuroscience* **106**, 313–330 (2001).
192. Chan, C. S. *et al.* HCN channelopathy in external globus pallidus neurons in models of Parkinson's disease. *Nat. Neurosci.* **14**, 85–92 (2011).
193. Leventhal, D. K. *et al.* Basal ganglia beta oscillations accompany cue utilization. *Neuron* **73**, 523–536 (2012).
194. Kuhn, A. A., Kupsch, A., Schneider, G. H. & Brown, P. Reduction in subthalamic 8-35 Hz oscillatory activity correlates with clinical improvement in Parkinson's disease. *Eur J Neurosci* **23**, 1956–60 (2006).
195. Gatev, P., Darbin, O. & Wichmann, T. Oscillations in the basal ganglia under normal conditions and in movement disorders. *Mov. Disord. Off. J. Mov. Disord. Soc.* **21**, 1566–1577 (2006).
196. Little, S. & Brown, P. The functional role of beta oscillations in Parkinson's disease. *Parkinsonism Relat. Disord.* **20 Suppl 1**, S44-48 (2014).
197. Stein, E. & Bar-Gad, I. β oscillations in the cortico-basal ganglia loop during parkinsonism. *Exp. Neurol.* **245**, 52–59 (2013).
198. Crompe, B. de la *et al.* The globus pallidus orchestrates abnormal network dynamics in a model of Parkinsonism. *Nat. Commun.* **11**, 1570 (2020).
199. Kovaleski, R. F. *et al.* Dysregulation of external globus pallidus-subthalamic nucleus network dynamics in parkinsonian mice during cortical slow-wave activity and activation. *J. Physiol.* **598**, 1897–1927 (2020).
200. Porter, R. H., Greene, J. G., Higgins, D. S. & Greenamyre, J. T. Polysynaptic regulation of glutamate receptors and mitochondrial enzyme activities in the basal ganglia of rats with unilateral dopamine depletion. *J. Neurosci. Off. J. Soc. Neurosci.* **14**, 7192–7199 (1994).
201. Betarbet, R., Porter, R. H. & Greenamyre, J. T. GluR1 glutamate receptor subunit is regulated differentially

- in the primate basal ganglia following nigrostriatal dopamine denervation. *J. Neurochem.* **74**, 1166–1174 (2000).
202. Starr, M. S., Starr, B. S. & Kaur, S. Stimulation of basal and L-DOPA-induced motor activity by glutamate antagonists in animal models of Parkinson's disease. *Neurosci. Biobehav. Rev.* **21**, 437–446 (1997).
203. Kelsey, J. E. *et al.* NMDA receptor antagonists ameliorate the stepping deficits produced by unilateral medial forebrain bundle injections of 6-OHDA in rats. *Psychopharmacology (Berl.)* **175**, 179–188 (2004).
204. Liu, J. *et al.* Facilitation of GluN2C-containing NMDA receptors in the external globus pallidus increases firing of fast spiking neurons and improves motor function in a hemiparkinsonian mouse model. *Neurobiol. Dis.* **150**, 105254 (2021).
205. Starr, P. A., Kang, G. A., Heath, S., Shimamoto, S. & Turner, R. S. Pallidal neuronal discharge in Huntington's disease: support for selective loss of striatal cells originating the indirect pathway. *Exp. Neurol.* **211**, 227–233 (2008).
206. Temel, Y. *et al.* Motor and cognitive improvement by deep brain stimulation in a transgenic rat model of Huntington's disease. *Neurosci. Lett.* **406**, 138–141 (2006).
207. Beste, C. *et al.* Behavioral and neurophysiological evidence for the enhancement of cognitive control under dorsal pallidal deep brain stimulation in Huntington's disease. *Brain Struct. Funct.* **220**, 2441–2448 (2015).
208. Reiner, A., Dragatsis, I. & Dietrich, P. Genetics and neuropathology of Huntington's disease. *Int. Rev. Neurobiol.* **98**, 325–372 (2011).
209. Waldvogel, H. J., Kim, E. H., Tippett, L. J., Vonsattel, J.-P. G. & Faull, R. L. M. The Neuropathology of Huntington's Disease. *Curr. Top. Behav. Neurosci.* **22**, 33–80 (2015).
210. Deng, Y., Wang, H., Joni, M., Sekhri, R. & Reiner, A. Progression of basal ganglia pathology in heterozygous Q175 knock-in Huntington's disease mice. *J. Comp. Neurol.* **529**, 1327–1371 (2021).
211. Waldvogel, H. J. & Faull, R. L. M. The diversity of GABA(A) receptor subunit distribution in the normal and Huntington's disease human brain. *Adv. Pharmacol. San Diego Calif* **73**, 223–264 (2015).
212. Perez-Rosello, T. *et al.* Enhanced striatopallidal gamma-aminobutyric acid (GABA)A receptor transmission in mouse models of huntington's disease. *Mov. Disord. Off. J. Mov. Disord. Soc.* **34**, 684–696 (2019).
213. Barry, J., Akopian, G., Cepeda, C. & Levine, M. S. Striatal Direct and Indirect Pathway Output Structures Are Differentially Altered in Mouse Models of Huntington's Disease. *J. Neurosci. Off. J. Soc. Neurosci.* **38**, 4678–4694 (2018).
214. Breakefield, X. O. *et al.* The pathophysiological basis of dystonias. *Nat. Rev. Neurosci.* **9**, 222–234 (2008).
215. Albanese, A. *et al.* Phenomenology and classification of dystonia: a consensus update. *Mov. Disord. Off. J. Mov. Disord. Soc.* **28**, 863–873 (2013).
216. Jinnah, H. A. & Factor, S. A. Diagnosis and treatment of dystonia. *Neurol. Clin.* **33**, 77–100 (2015).
217. Schwarz, C. S. & Bressman, S. B. Genetics and treatment of dystonia. *Neurol. Clin.* **27**, 697–718, vi (2009).
218. Tanabe, L. M., Kim, C. E., Alagem, N. & Dauer, W. T. Primary dystonia: molecules and mechanisms. *Nat. Rev. Neurol.* **5**, 598–609 (2009).
219. Starr, P. A. *et al.* Spontaneous pallidal neuronal activity in human dystonia: comparison with Parkinson's

- disease and normal macaque. *J. Neurophysiol.* **93**, 3165–3176 (2005).
220. Chiken, S., Shashidharan, P. & Nambu, A. Cortically evoked long-lasting inhibition of pallidal neurons in a transgenic mouse model of dystonia. *J. Neurosci. Off. J. Soc. Neurosci.* **28**, 13967–13977 (2008).
221. Baron, M. S., Chaniary, K. D., Rice, A. C. & Shapiro, S. M. Multi-neuronal recordings in the Basal Ganglia in normal and dystonic rats. *Front. Syst. Neurosci.* **5**, 67 (2011).
222. Nambu, A. *et al.* Reduced pallidal output causes dystonia. *Front. Syst. Neurosci.* **5**, 89 (2011).
223. Nishibayashi, H. *et al.* Cortically evoked responses of human pallidal neurons recorded during stereotactic neurosurgery. *Mov. Disord. Off. J. Mov. Disord. Soc.* **26**, 469–476 (2011).
224. Sciamanna, G. *et al.* Optogenetic Activation of Striatopallidal Neurons Reveals Altered HCN Gating in DYT1 Dystonia. *Cell Rep.* **31**, 107644 (2020).
225. Seroogy, K. B. *et al.* Dopaminergic neurons in rat ventral midbrain express brain-derived neurotrophic factor and neurotrophin-3 mRNAs. *J. Comp. Neurol.* **342**, 321–334 (1994).
226. Gonzalez-Reyes, L. E. *et al.* Sonic hedgehog maintains cellular and neurochemical homeostasis in the adult nigrostriatal circuit. *Neuron* **75**, 306–319 (2012).

Figure Legends (1452 words)

Figure 1. Cellular and circuit substrates for motor regulation by the GPe.

- a.** A simplified circuit diagram showing the key nodes within the basal ganglia. The dorsal striatum and subthalamic nucleus are the two input stations that receive excitatory cortical inputs; the substantia nigra pars reticulata is the output station that provides inhibitory projection to the thalamus. The entire basal ganglia circuit, especially the dorsal striatum, is under the neuromodulatory control of the substantia nigra pars compacta. Size of the target areas (circles) is an artistic rendering based on the volume of the brain areas. The circuit role of the GPe is often ignored.
- b.** A modified circuit model highlighting the central role of the GPe within the basal ganglia. The GPe sends inhibitory projections to all key structures within the circuit.
- c.** Pie chart summarizing the neuronal composition of the mouse GPe. The area of the sectors represents the approximate size of each neuron class. PV⁺ neurons (which constitute 50% of the GPe) are heterogeneous and assume the canonical role of the GPe by projecting to the subthalamic nucleus and substantia nigra pars reticulata. Npas1⁺ neurons are 30% of the GPe; they can be subdivided into two subclasses (see **f**). Consistent with the distinct electrophysiological properties, PV⁺ neurons and Npas1⁺ neurons have unique behavioral roles: PV⁺ neurons are motor-promoting, while Npas1⁺ neurons are motor-inhibiting. PV⁺ neuron and Npas1⁺ neuron classes jointly tune motor behavior through a push-pull mechanism. Local inhibitory connections between these neuron classes may control this process. ChAT⁺ neurons are ~5% of the total GPe neuron population and show no overlap with other known classes of GPe neurons. They project broadly to cortical areas. PV⁻-Npas1⁻ neurons amount to ~15% of the total GPe and are the least characterized neuron subtype.

d. Single-cell transcriptomic data identify four distinct clusters of GPe neurons; these include Npas1⁺-Foxp2⁺ (blue, 10 o'clock), Npas1⁺-Nkx2.1⁺ (cyan, 7 o'clock), and two subpopulations of PV⁺ neurons (red and teal, 6 o'clock). Data adapted from Saunders et al.,⁷. Original expression data can be viewed at http://dropviz.org/?_state_id_=6c13807c8420bc74.

e. GPe neuron subtypes display distinct electrophysiological properties. Heatmap representation of electrical signatures of genetically-identified GPe neuron subtypes. Dendrograms show the order and distances of neuron clusters and their electrical characteristics. A total of 212 neurons ($n = \text{Dbx1}^+ : 20, \text{Foxp2}^+ : 16, \text{Kcng4}^+ : 13, \text{Lhx6}^+_{\text{bright}} : 18, \text{Lhx6}^+_{\text{dim}} : 7, \text{PV}^+ : 38, \text{PV}^+ \text{-Dbx1}^+ : 16, \text{PV}^+ \text{-Lhx6}^+ : 12, \text{PV}^+ \text{-Npy2r}^+ : 21, \text{Npas1}^+ : 19, \text{Npas1}^+ \text{-Lhx6}^+ : 13, \text{Npr3}^+ : 8, \text{Npy2r}^+ : 10$) were included in this analysis. Neurons with incomplete data were excluded from the analysis. Two main clusters were identified; cluster 1 contains 87 cells, cluster 2 contains 125 cells. Column labels (left to right): membrane potential, CV_{ISI} , sag ratio, spike width, spike height, first/last ISI ratio, basal activity, trough potential, max rate, and max current. Data adapted from Cui et al.,⁴⁴. The complete dataset for electrophysiological measurements of the intrinsic properties and an interactive web tool can be found online: https://icbi-georgetown.shinyapps.io/Neuro_interactive_analysis/. Abbreviations: LGE, lateral ganglionic eminence; MGE, medial ganglionic eminence.

f. Efferent projections of principal GPe neuron subtypes. Two *bona fide* subclasses of Npas1⁺ neurons are identified in the mouse GPe. They differ in their molecular marker expression, axonal projections, and electrophysiological properties. Npas1⁺-Foxp2⁺ neurons represent 60% of the total Npas1⁺ neuron class; they project exclusively to the dorsal striatum, targeting spiny projection neurons. Npas1⁺-Nkx2.1⁺ neurons represent 40% of the total Npas1⁺ neuron class; they project to the cortex, thalamus, and midbrain. Npas1⁺-Foxp2⁺ neurons alone are sufficient to account for the motor-suppressing effect produced by optogenetic stimulation of pan-Npas1⁺ neurons *in vivo*. In contrast, the behavioral roles of Npas1⁺-Nkx2.1⁺ awaits further clarification. In addition, at least two subclasses of PV⁺ neurons are identified. The characteristics of PV⁺-Kcng4⁺ neurons overlap with that of canonical PV⁺ neurons, while the PV⁺-Lhx6⁻ neurons project to the thalamic parafascicular nucleus. Size of the target areas (circles) is an artistic rendering based on the volume of the target areas, and does not reflect the axonal density, synaptic strength, or contacts formed by Npas1⁺ neuron subclasses.

Figure 2. Organization of striatopallidal projections.

a. Top: representative two-photon images from coronal sections showing GPe-projecting neurons found in the dorsal striatum (dStr). Inset indicates the location of the injection site. Bottom: unbiased quantification of GPe-projecting neurons across the entire brain. Each marker represents a mouse ($n = 8$ mice). The arrow points to the data (red) from the dStr. Abbreviations: BLA, basolateral amygdalar nucleus; BSTa, bed nuclei of the stria terminalis, anterior division; cc, corpus callosum; CeA, central amygdala; CLA, claustrum; cpd, cerebral peduncle; Ctx, cortex; DR, dorsal raphe nucleus; dStr, dorsal striatum; fr, fasciculus retroflexus; GPe, external globus pallidus; GPi, internal globus pallidus; GU, gustatory areas; MOp, primary motor area; MOs, secondary motor area; MRN, midbrain reticular nucleus; opt, optic tract; PAG, periaqueductal gray; PF, parafascicular nucleus; PO, posterior complex of the thalamus; PPN, pedunculopontine nucleus; PRNc, pontine reticular nucleus, caudal part; PRNr,

pontine reticular nucleus, rostral part; SCm, superior colliculus, motor related; SI, substantia innominata; SNc, substantia nigra pars compacta; SNr, substantia nigra pars reticulata; SSp-bfd, primary somatosensory area, barrel field; SSp-ll, primary somatosensory area, lower limb; SSp-m, primary somatosensory area, mouth; SSp-n, primary somatosensory area, nose; SSp-tr, primary somatosensory area, trunk; SSp-ul, primary somatosensory area, upper limb; SSp, supplemental somatosensory area; STN, subthalamic nucleus; VAL, ventral anterior-lateral complex of the thalamus; VISC, visceral area; VM, ventromedial thalamic nucleus; VPM, ventral posteromedial thalamic nucleus; Th, thalamus; ZI, zona incerta. Data adapted from Cui et al.,⁸¹.

b. Grayscale representation showing eGFP signals from CreOn-mRuby2-T2A-Synaptophysin-eGFP AAV injections into the dorsomedial striatum (DMS) or dorsolateral striatum (DLS) of *Adora2a*^{Cre} (left) and *Drd1a*^{Cre} (right) mice. dSPNs and iSPNs from the DMS and DLS send projections to the medial and lateral portions of the GPe. Data adapted from Cui et al.,⁸¹.

c. Left: The anatomical arrangement of the dStr-GPe synapse is illustrated in an electron micrograph (adapted from Galvan et al.,⁷⁹). Striatal terminals (light blue) are sandwiched between GPe dendrites (pink) and astrocytic processes (brown; black arrows). Right, top: morphological reconstructions of Alexa-filled GPe astrocytes in a naïve mouse (top). Right, bottom: Sholl diagram of Alexa-filled and reconstructed astrocytes in naïve mice (black) and chronic 6-OHDA lesioned mice (red). Data are shown as the number of intersections at 1- μ m eccentricities from the soma. Population means and their difference (gray) was highlighted. Data adapted from Cui et al.,⁷⁵ (see also **Box 3**).

Figure 3. Functional analysis of GPe neurons.

a. Optogenetic stimulation of PV⁺ neurons promotes locomotion. Left: A plot showing the relationship between normalized speed and time. Blue bar indicates the duration (10 s) of light delivery. The dotted horizontal line indicates the baseline locomotor activity level. Black solid trace is the population mean calculated from all mice; shading indicates the standard error of the mean. Black dotted trace is a representative example from a single mouse; data were scaled to facilitate comparison. Right: Speed during 'light-period' against speed during 'pre-period' is plotted. Data from PV-Cre mice expressing ChR2-eYFP (circles) and eYFP (crosses) are displayed. Each marker represents a mouse. The diagonal line indicates unity (i.e., $x = y$). Data points for ChR2-eYFP are systematically shifted upwards relative to unity. Data adapted from Pamukcu et al.,³⁸.

b. Optogenetic stimulation of Npas1⁺ neurons suppresses locomotion (same protocol as in **a**). Data from Npas1-Cre-tdTomato mice expressing ChR2-eYFP (circles) and eYFP (crosses) are displayed. Data adapted from Pamukcu et al.,³⁸.

c. Left: representative dF/F traces of GCaMP6s signal (green) recorded from axonal fibers of SNr-projecting PV⁺ neurons and corresponding treadmill velocity (gray) during head-fixed, self-initiated motor behavior. Right: mean acceleration (black), velocity (gray) and z-scored dF/F triggered at locomotion initiations and terminations (mean across all events). Data adapted from Lilascharoen et al.,⁵².

d. Heatmap summarizing motor responses of mice to optogenetic stimulation of genetically-defined neurons in the GPe. Twenty-five movement metrics were measured to fully capture the behavioral structures. Each of the 25

rows represents the fold change of movement metrics. Warm colors (red) represent positive changes; cool colors (blue) represent negative changes. Rows and columns are sorted using hierarchical clustering. Dendrograms are divided into two main arms; metrics on the upper arm are negatively correlated with 'total frequency', while metrics on the lower arm are positively correlated with 'total frequency'. Each column is a mouse; 54 mice were used in this analysis. The neurons of interest are PV⁺ (purple), Npas1⁺ (green), Kcng4⁺ (blue), and Foxp2⁺ (red) neurons. Data adapted from Cui et al.,⁴⁴.

e. Optogenetic inhibition of GPe neurons induces β -oscillations. Mean normalized power spectrum of motor cortex electrocorticogram (ECoG) during off (black) and on (red) laser stimulations. Data adapted from de la Crompe et al.,¹⁹⁸.

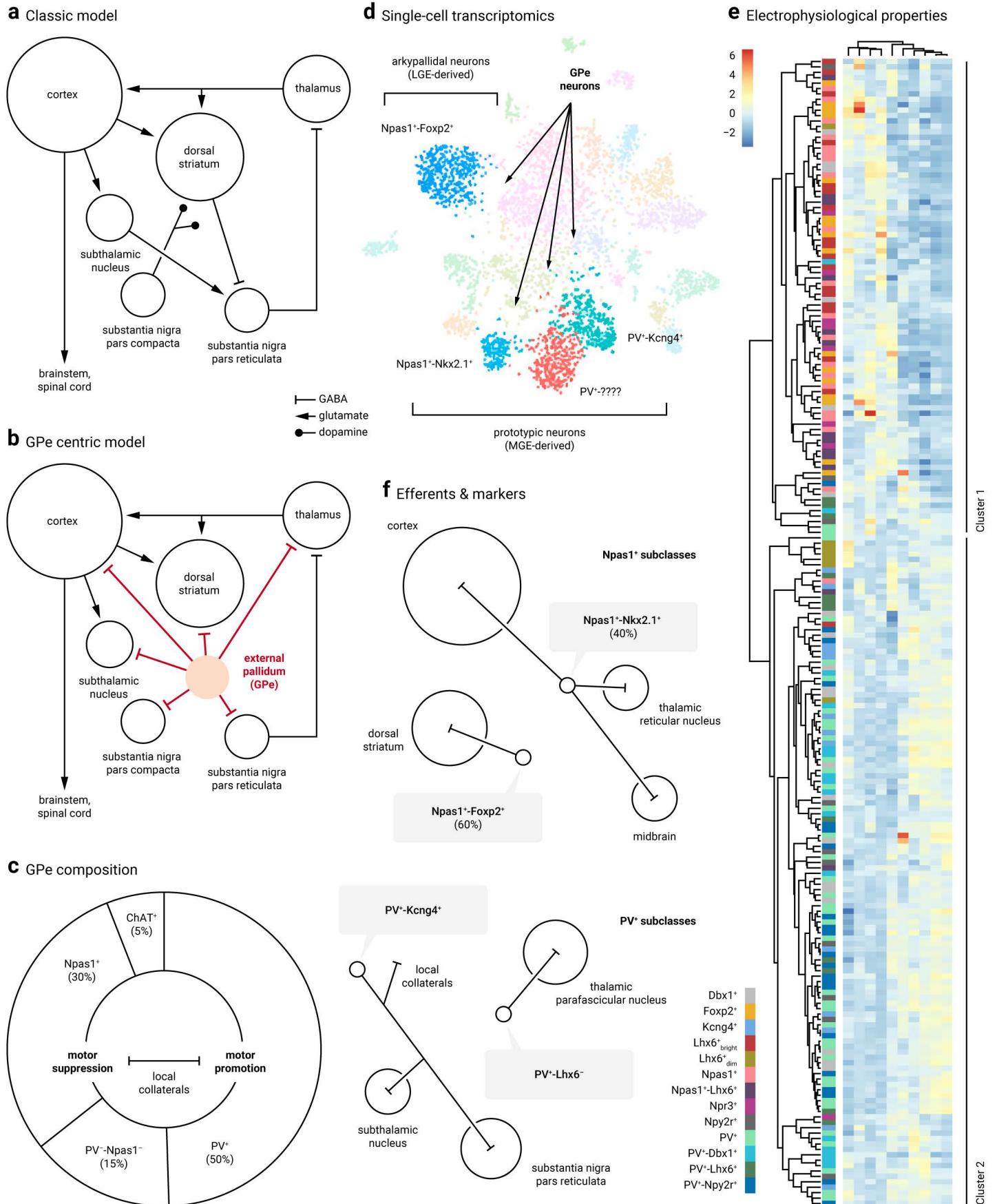
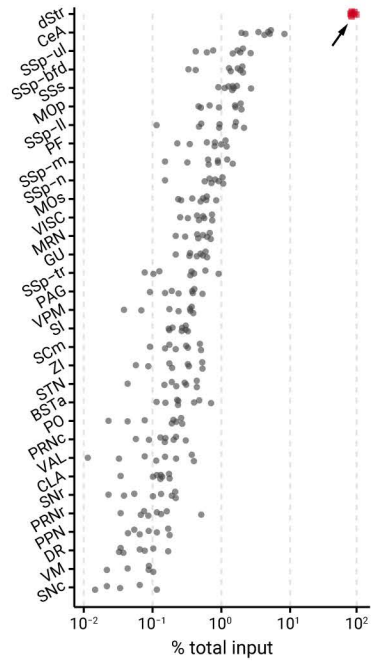
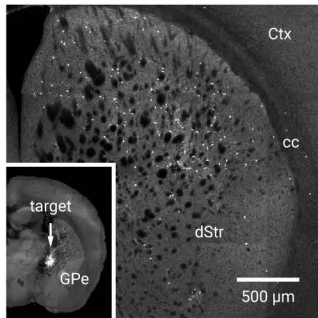
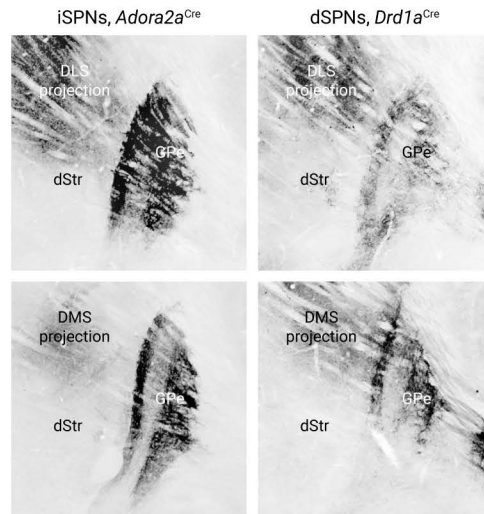


Figure 1

a Whole-brain inputs



b Topographical dStr-GPe projection



c Glial ensheathment

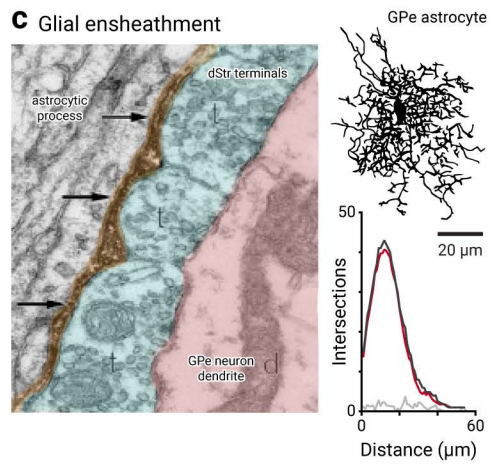


Figure 2

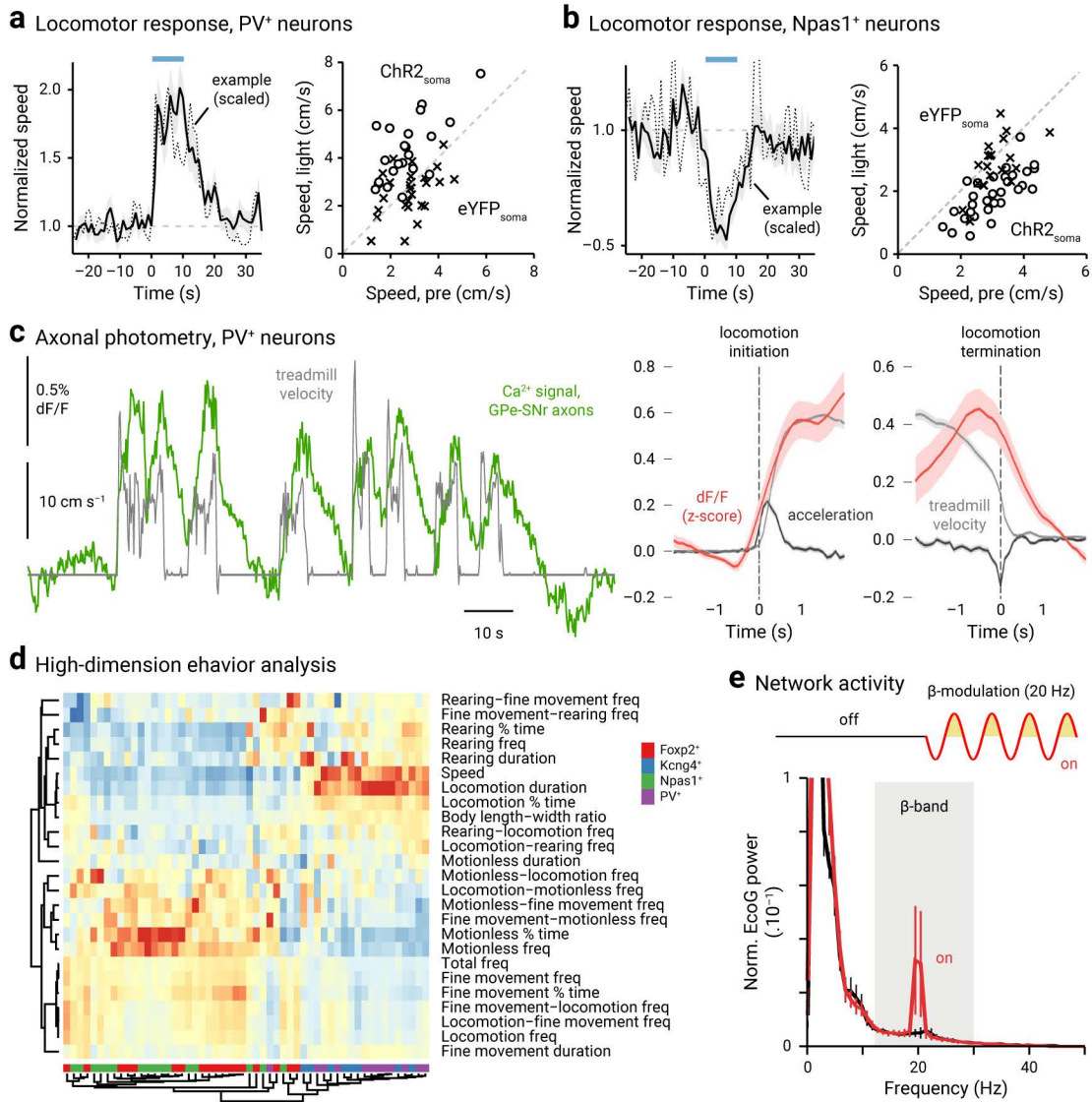


Figure 3